EL4 cells (ATCC: TIB-39) and E.G7-OVA cells (ATCC: CRL-2113) were purchased from the American Type Culture Collection (ATCC, Manassas, VA, USA) and maintained in Dulbecco's modified Eagle's medium supplemented with 10% FBS and RPMI 1640 supplemented with 10% FBS, 4.5 g/l glucose, 10 mM HEPES, 1 mM sodium pyruvate, 0.05 mM 2-mercaptoethanol and 0.4 mg/ml G418.

Synthesis of Man-C4-Chol and Gal-C4-Chol

Man-C4-Chol and Gal-C4-Chol were synthesized as described previously [19,22]. Briefly, *N*-(4-aminobutyl)-(cholesten-5-yloxyl)formamide (C4-Chol) was synthesized from cholesteryl chloroformate and *N*-(4-aminobutyl)carbamic acid *tert*-butyl ester. The C4-Chol was reacted with 5 equivalents of 2-imino-2-methoxyethyl-1-thiomannoside or 2-imino-2-methoxyethyl-1-thiogalactoside [27] in pyridine containing 1.1 equivalents of triethylamine for 24 h. After evaporation of the reaction mixture *in vacuo*, the resultant material was suspended in water and dialyzed against water for 48 h, and then lyophilized.

Construction and preparation of pCMV-OVA

pCMV-OVA was constructed by subcloning the EcoRI chicken egg albumin (ovalbumin) cDNA fragment from pAc-neo-OVA [28], which was kindly provided by Dr. M. J. Bevan (University of Washington, Seattle, WA, USA), into the polylinker of pVAX I. pCMV-OVA was amplified in the *E. coli* strain, DH5α, then isolated, and purified using a Qiagen plasmid giga kit (Qiagen GmbH, Hilden, Germany). The endotoxin in pCMV-OVA solution was removed by the Triton X-114 method.

Preparation of cationic liposomes

Liposomes were prepared using the method reported previously [19,22]. Briefly, DOTMA, Chol, and Man-C4-Chol or Gal-C4-Chol were mixed in chloroform at a molar ratio of 2:1:1:0, 2:1:0:1, and 2:2:0:0 to prepare Man-liposomes, Gal-liposomes, and cationic liposomes, respectively. Then, the mixture was dried, vacuum desiccated, and resuspended in sterile 20 mM HEPES buffer (pH 7.8) or 5% dextrose solution in a sterile test tube for *in vitro* and *in vivo* experiments, respectively. After hydration, the dispersion was sonicated for 5 min in a bath sonicator to produce liposomes and then sterilized by passing through a 0.45 μm filter (Nihon-Millipore Ltd., Tokyo, Japan).

Preparation of lipoplex for *in vitro* study

Lipoplex was prepared using the method reported previously [19,22]. Briefly, equal volumes of pCMV-OVA and stock liposome solution were diluted with Opti-MEM I® in 15 ml Falcon tubes. Then, pCMV-OVA solution was added rapidly to the surface of the liposome solution at a charge ratio (−/+) of 1.0 : 2.3 using a micropipette (Pipetman®, Gilson, Villier-le Bel, France) and the mixture was agitated rapidly by pumping it up and down twice in the pipette tip.

Preparation of lipoplex for *in vivo* study

All cationic liposome/pCMV-OVA complexes for *in vivo* experiments were prepared under the optimal conditions for cell-selective gene transfection as reported previously [29–31]. Briefly, equal volumes of pCMV-OVA and stock liposome solution were diluted with 5% dextrose in 15 ml tubes. Then, pCMV-OVA solution was added rapidly to the surface of the liposome solution using a micropipette and the mixture was agitated rapidly by pumping it up and down twice in the pipette tip. The mean particle sizes were measured by dynamic light scattering spectrophotometry (LS-900; Otsuka Electronics Co., Ltd., Osaka, Japan). The zeta-potential of the lipoplexes was measured by the laser-Doppler electrophoresis method with a Zetasizer Nano ZS (Malvern Instruments Ltd., Worcestershire, UK).

Uptake characteristics by DC2.4 cells

Uptake study was performed by the method reported previously [19,22]. Briefly, the DC2.4 cells were plated on a 24-well plate at a density of 0.65×10^5 cells/cm^2 and cultivated in 500 μl RPMI supplemented with 10% FBS. Twenty-four hours later, the culture medium was replaced with an equivalent volume of Hanks medium (Nissui Pharmaceutical Co., Ltd., Tokyo, Japan) containing 1 kBq/ml [^{32}P]-pCMV-OVA, 0.5 mg/ml cold pCMV-OVA and cationic liposomes at a charge ratio (−/+) of 1.0 : 2.3. After incubation for given time periods, the solution was quickly removed by aspiration, the cells were washed five times with ice-cold HBSS buffer and then solubilized in 0.3 M NaOH solution with 10% Triton X-100 (0.3 ml). The radioactivity was measured by liquid scintillation counting (LSC-500; Beckman, Inc., Tokyo, Japan) and the protein content was determined by a modification of the Lowry method. The effect of the presence of 0.125 mg/ml mannan was determined in the same system.

Transfection activity by DC2.4 cells

DC2.4 cells were seeded in 10.5 cm^2 dishes at a density of 0.65×10^5 cells/cm^2 in RPMI 1640 medium supplemented with 10% FBS. After 24 h in culture, the culture medium was replaced with Opti-MEM I® containing 0.5 μg/ml pCMV-OVA and cationic liposomes. Six hours later, the incubation medium was replaced again with RPMI 1640 supplemented with 10% FBS and incubated for an additional 6 h. Then, the cells were

scraped and suspended in 200 μl pH 7.4 phosphate-buffered saline (PBS). Total RNA was isolated from DC2.4 cells with MagExtractor MFX-2000 (Toyobo Co., Ltd., Osaka, Japan) and MagExtractor-RNA following the manufacturer's instructions. Reverse transcription of mRNA was carried out using a first strand cDNA synthesis kit as follows: total RNA was added to the oligo dT primer (0.8 μg/μl) solution, and incubated at 42 °C for 60 min with a program temperature control system PC-808 (Astec Co., Ltd., Fukuoka, Japan). Real-time PCR was performed using the Lightcycler™ quick system 350S (Roche Diagnostics Co., Indianapolis, IN, USA) with hybridization probes. Primer and hybridization probes for OVA cDNA were constructed as follows: primer, 5′-GCGTCTCTGAATTTAGGG-3′ (forward) and 5′-TACCCCTGATACTACAGTGC-3′ (reverse); hybridization probes, 5′-CTTCTGTATCAAGCACATCGCAACCAACG-3′-fluorescein isothiocyanate (FITC) and Lightcycler™-Red640 (LCRed)-5′-CGTTCTCTTCTTTGGCAGATGTGT-TTCCCC-3′. The PCR reaction for detection of the OVA gene was carried out in a final volume of 20 μl containing: (i) 2 μl DNA Master hybridization probes 10× (DNA Master hybridization probes kit); (ii) 1.6 μl 25 mM $MgCl_2$; (iii) 1.5 μl forward and reverse primers (final concentration 0.75 μM); (iv) 1 μl 2 μM FITC-labeled hybridization probes and 2 μl 2 μM LCRed-labeled probes (final concentrations 0.2 and 0.4 μM, respectively); (v) 5.4 μl H_2O; (vi) 5 ml cDNA or pCMV-OVA solution. For the mouse β-actin cDNA measurements, samples were prepared in accordance with the instruction manuals. After an initial denaturation step at 95 °C for 10 min, temperature cycling was initiated. Each cycle consisted of denaturation at 95 °C for 10 s, hybridization at 60 °C for 15 s, and elongation at 72 °C for 10 s. The fluorescent signal was acquired at the end of the hybridization step (F2/F1 channels). The total number of cycles performed was 40. The mRNA copy numbers were calculated for each sample from the standard curve using the instrument software ('Arithmetic Fit Point analysis' for the Lightcycler). Results were expressed as relative copy numbers calculated relative to β-actin mRNA (copy number of OVA mRNA/copy number of β-actin mRNA).

Quantification of OVA mRNA in CD11c$^+$ cells after i.p. administration by quantitative PCR

pCMV-OVA (100 μg) or lipoplex was injected via the i.p. route. Spleens and peritoneal cells were harvested 6 h after i.p. administration and single cell suspensions of spleen cells were prepared in ice-cold RPMI 1640 medium. Ice-cold RPMI 1640 medium (5 ml) was injected and then peritoneal cells were collected as a cell suspension in RPMI medium. Following this, red blood cells were removed by incubation with Tris-NH_4Cl solution for 10 min at room temperature. Positive selection of CD11c$^+$ cells was carried out by magnetic cell sorting with auto MACS (Miltenyi Biotec Inc., Auburn, CA, USA) following the manufacturer's instructions. Briefly, the cell suspension was incubated with PBS containing 1 mg/ml IgG to block the Fcγ receptors of macrophages. Then, CD11c$^+$ cells were labeled by incubating with anti-CD11c monoclonal antibody (N418)-labeled magnetic beads. After washing three times, CD11c$^+$ cells were collected by auto MACS. Total RNA was isolated from the recovered CD11c$^+$ cells with a MagExtractor MFX-2000 (Toyobo Co., Ltd., Osaka, Japan) and MagExtractor-RNA following the manufacturer's instructions. Reverse transcription and quantitative PCR of OVA and β-actin mRNA were performed as described in the section 'Transfection activity by DC2.4 cells'.

Induction of OVA-specific CTL

C57BL/6 mice were immunized with naked pCMV-OVA (50 or 100 μg) or lipoplexes by i.p., i.m., or intradermal (i.d.) administration three times at intervals of 2 weeks. Two weeks after the last immunization, the spleens of each group were harvested and a single cell suspension was prepared in ice-cold RPMI 1640 medium. Then, the spleen cells were resuspended in RPMI 1640 medium supplemented with 10% FBS and 2-mercaptoethanol. The recovered spleen cells were plated in a 25-cm flask at 5×10^6 cells/ml along with MMC and E.G7-OVA cells and treated for 1 h (100 μg/ml, 1 h). Four days after cultivation, non-adherent cells were harvested, washed, and plated with relevant or irrelevant target cells at effector/target (E/T) ratios of 100 : 1, 50 : 1, 25 : 1, and 12.5 : 1. The target cells were E.G7-OVA cells or their parental cell line, EL4 cells. The target cell (E.G7-OVA or EL4 cells) suspensions in RPMI medium (2.5×10^7 cells/ml) were incubated with ^{51}Cr (7.4 MBq/ml) for 1 h. Following incubation, the cells were washed five times and then resuspended at 2×10^5 cells/ml. The target cells (E.G7-OVA or EL4 cells; 2×10^4 cells) were added to each well of a 96-well microtiter plate, along with 2×10^6, 1×10^6, 5×10^5, or 2.5×10^5 spleen cells and the plates were mixed and incubated for 4 h at 37 °C and 5% CO_2 in an incubator. After further centrifugation, 100 μl supernatant was collected from each well and the radioactivity released was measured in a gamma counter. The percentage ^{51}Cr release was calculated as follows: specific lysis (%) = [(experimental ^{51}Cr release − spontaneous ^{51}Cr release)/(maximum ^{51}Cr release − spontaneous ^{51}Cr release)] × 100). The percentage OVA-specific ^{51}Cr release was calculated as (% of ^{51}Cr release from E.G7-OVA) − (% of ^{51}Cr release from EL4).

Evaluation of protection against transplanted tumor cells in mice

C57BL/6 mice were immunized three times by i.p. or i.m. administration of naked pCMV-OVA (100 μg) or lipoplex at 2-week intervals. Then 2 weeks after the last

immunization, E.G7-OVA (1×10^6) or EL4 (1×10^6) cells were inoculated subcutaneously (s.c.) into the back of the mice. The survival of the mice was monitored up to 100 days after inoculation of the E.G7-OVA or EL4 cells.

Results

Particle sizes and zeta-potentials of Man-lipoplexes

To investigate the physicochemical properties of lipoplexes, the particle size and zeta-potential of each lipoplex were evaluated. Both lipoplexes showed a clear-cut distribution pattern and the mean particle sizes of the Man-lipoplexes and conventional lipoplex were 114 ± 7.8 and 116 ± 11.5 nm ($n = 3$), respectively. Zeta-potential analysis showed that the zeta-potential of the Man-lipoplex and the conventional lipoplex at a charge ratio (−/+) of 1.0 : 2.3 was 62.1 ± 1.85 and 64.1 ± 1.74 mV ($n = 3$), respectively. These results show that there was almost no difference in physicochemical properties between the two complexes. The galactosylated lipoplex (Gal-lipoplex) also showed a similar size distribution and zeta-potential (data not shown).

Uptake characteristics of Man-lipoplex by DC2.4 cells *in vitro*

To evaluate the potency of the Man-lipoplex in terms of targeted delivery to DCs, the uptake of the lipoplexes and subsequent transfection to cells were evaluated. In this study, we used DC2.4 cells, a cell line derived from DCs, as a model DC expressing mannose receptors [26]. The [^{32}P] Man-lipoplex was taken up by DC2.4 cells more efficiently than the conventional [^{32}P] lipoplex (Figure 1a) and this was significantly reduced in the presence of an excess of mannan (Figure 1b). In contrast, the uptake with conventional lipoplex was not significantly inhibited by an excess of mannan (Figure 1b).

Transfection characteristics of Man-lipoplex with respect to DC2.4 cells *in vitro*

We next investigated the transfection activity of the Man-lipoplex with respect to DC2.4 cells. As shown in Figure 2a, the highest gene expression was observed in the Man-lipoplex. In the presence of an excess of mannan, the gene expression of the Man-lipoplex was significantly inhibited (Figure 2b). In contrast, the gene expression with conventional lipoplex and naked pDNA was not significantly inhibited in the presence of an excess of mannan (Figure 2b).

Effect of Man-lipoplex administration routes on CTL response

To investigate the effect of the administration route of the Man-lipoplex, the induction of an OVA-specific cytotoxic response with a ^{51}Cr release assay using E.G7-OVA cells (OVA-expressing cells), and its parental cell line, EL4 cells (OVA-non-expressing cells), was examined. We found that the CTL activity induced by i.p. administration of the Man-lipoplex was higher than that induced by i.m. or i.d. administration of the Man-lipoplex (Figure 3a).

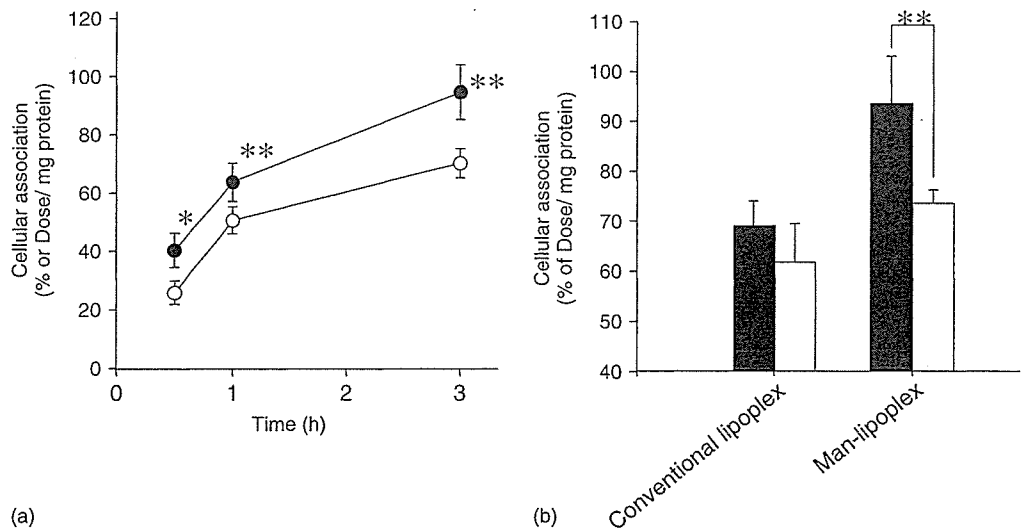

Figure 1. Cellular association of the Man-lipoplex in DC2.4 cells. (a) Cellular association time-course of ^{32}P-labeled Man-lipoplex (●) and lipoplex (○) in DC2.4 cells at 37 °C. pCMV-OVA (0.5 μg/ml) was complexed with cationic liposomes at a charge ratio (−/+) of 1.0 : 1.6. Each value represents the mean ± standard deviation (S.D.) ($n = 3$). (b) Cellular association of ^{32}P-labeled lipoplex or Man-lipoplex in the absence (■) or presence (□) of 0.125 mg/ml mannan in the culture medium. Each value represents the mean + S.D. ($n = 4$). Statistical analysis was performed by Student's *t*-test (*$P < 0.05$, **$P < 0.01$)

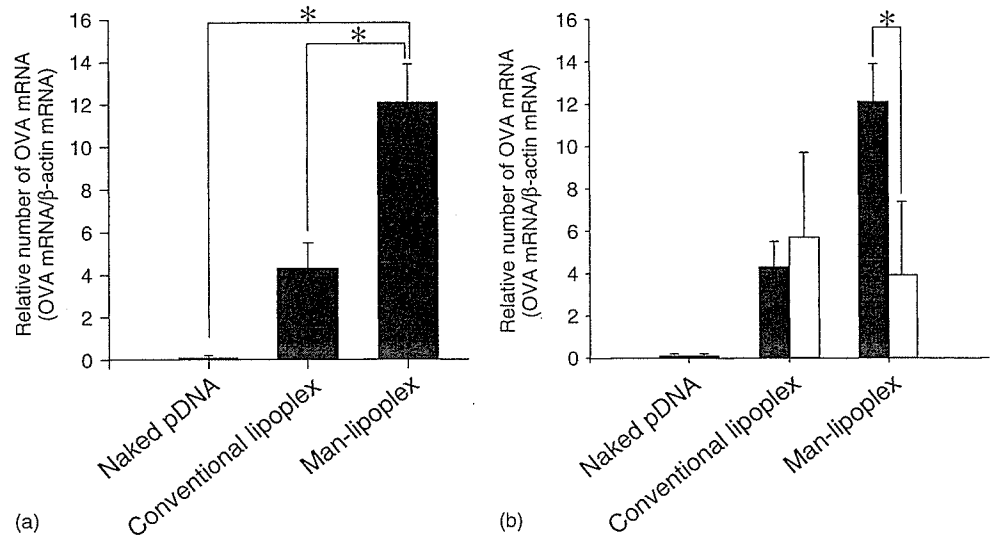

Figure 2. Transfection activity of the Man-lipoplex in DC2.4 cells. (a) Transfection activity of naked pCMV-OVA or lipoplexes in cultured DC2.4 cells. The concentration of pDNA was fixed at 0.5 μg/ml in all experiments. Each value represents the mean + S.D. (n = 3). (b) Transfection activity of naked pCMV-OVA or lipoplexes in the absence (■) or presence (□) of 0.125 mg/ml mannan. The concentration of pCMV-OVA was fixed at 0.5 μg/ml in all experiments. Each value represents the mean + S.D. values (n = 4). Statistical analysis was performed by analysis of variance (*$P < 0.05$)

Furthermore, increasing the amount of pCMV-OVA of the Man-lipoplex markedly enhanced the CTL response induced by i.p. administration (Figure 3b). Furthermore, the CTL activity of the Man-lipoplex following i.p. administration was significantly higher than that induced by i.m. administration of naked pCMV-OVA (Figure 3c).

Effect of lipoplex mannosylation on CTL response

As shown in Figure 4a, the Man-lipoplex induced a much higher CTL response than the conventional lipoplex. However, the Gal-lipoplex induced a much lower CTL response than the Man-lipoplex (Figure 4b), suggesting that the Man-lipoplex induces a strong CTL response via a mannose receptor-mediated mechanism.

Gene expression characteristics of Man-lipoplex on CD11c$^+$ cells in the spleen and peritoneal cavity after i.p. administration

To clarify the transfection activity of the Man-lipoplex with regard to DCs after i.p. administration, the OVA mRNA in the CD11c$^+$ cells in the spleen and peritoneal cavity was determined 6 h after i.p. administration of naked pCMV-OVA (100 μg) or Man-lipoplex and conventional lipoplex using quantitative RT-PCR. The relative copy number of OVA mRNA in the Man-lipoplex injected group was the highest of all in both peritoneal CD11c$^+$ cells (Figure 5a) and splenic CD11c$^+$ cells (Figure 5b).

Anti-tumor responses of Man-lipoplex after immunization

To assess the protective anti-tumor effect, EL4 and E.G7-OVA cells were transplanted into pre-immunized mice. Pre-immunization with the Man-lipoplex prolonged the survival time after transplantation of E.G7-OVA cells compared with pDNA or conventional lipoplex (Figure 6a). However, all formulations failed to prolong the survival rate after transplantation of EL4 cells (Figure 6b).

Discussion

DNA vaccine represents an exciting novel approach in vaccine development. The vaccine construct is created by insertion of a DNA encoding the desired antigen into a pDNA. The extent to which the pDNA is able to transfect cells is dependent on the application route and delivery carrier used. The encoded protein is then expressed in the transfected cells *in vivo* and, consequently, an immune response is elicited to the expressed antigen. However, to date, there have been few reports on *in vivo* gene therapy based on targeted non-viral gene delivery. In our series of experiments, we have been developing APC-selective *in vivo* gene carrier systems for use in gene therapy [22–24,32]. In the present study, we describe the Man-lipoplex given i.p. as a novel approach to enhance therapeutic potency of DNA vaccine therapy *in vivo*.

Since some clinical trials have involved the local administration of naked pDNA [7–9], we evaluated the OVA-specific CTL response following the local administration of naked pDNA. As shown in Figure 3c,

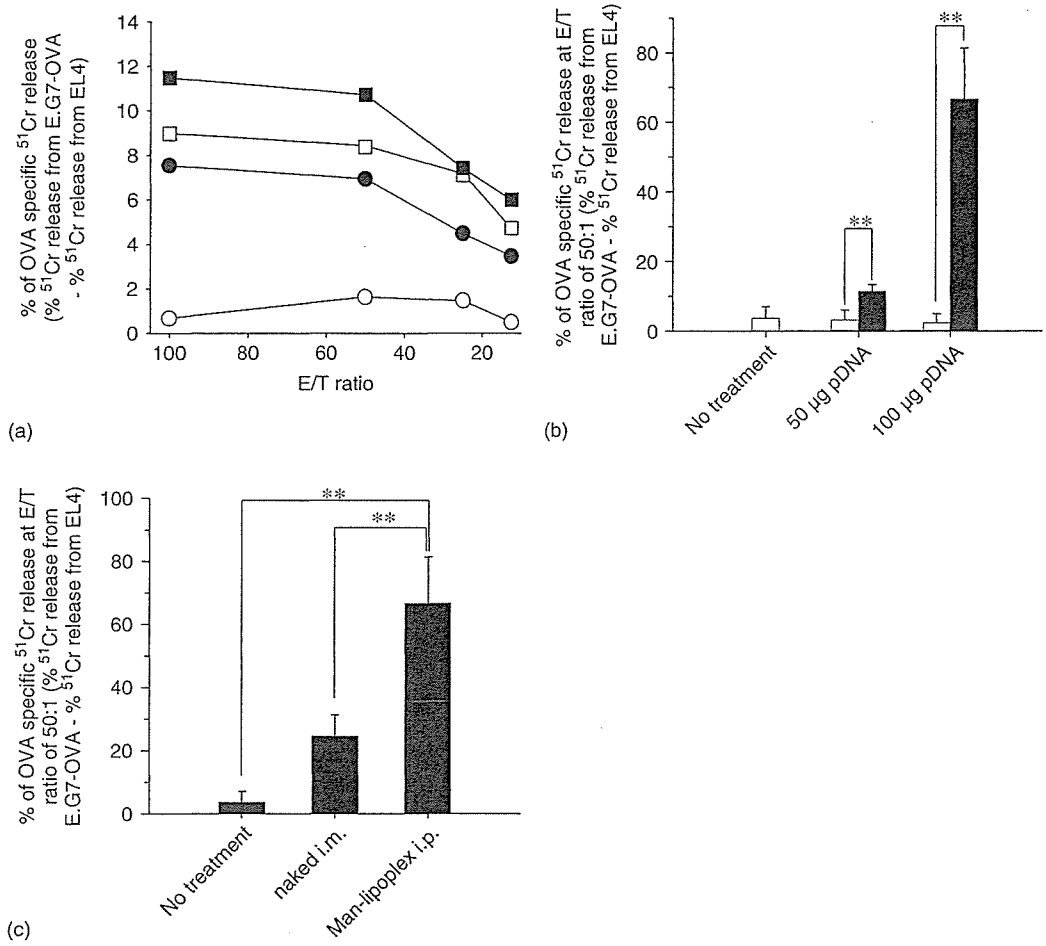

Figure 3. Effect of the route of administration and dose on immunization with naked pCMV-OVA or Man-lipoplexes. Mice were injected with 50 μg pCMV-OVA as naked pCMV-OVA or Man-lipoplexes biweekly three times before the experiment. (a) CTL activity primed by i.p. (■), i.d. (□) and i.m. (●) administration of the Man-lipoplexes or CTL activity in the no-treatment group (○). OVA-specific cell lysis at various effector/target (E/T) ratios was calculated from the % ^{51}Cr release from EL4 cells and from E.G7-OVA cells. Each value represents the mean of 4–5 experiments. (b) CTL response induced by the Man-lipoplexes (■) and naked pCMV-OVA (□) given i.p. at a dose of 50 or 100 μg/mouse. OVA-specific ^{51}Cr release at an E/T ratio of 50 : 1 was calculated from the following equation: OVA-specific ^{51}Cr release = %^{51}Cr release from E.G7-OVA cells −%^{51}Cr release from EL4 cells. Each value represents the mean + S.D. (control group: n = 3, other groups: n = 5). Statistical analysis was performed by analysis of variance (**$P < 0.01$). (c) CTL response induced by the Man-lipoplexes given i.p. and naked pCMV-OVA given i.m. at a dose of 50 or 100 μg/mouse. OVA-specific ^{51}Cr release at an E/T ratio of 50 : 1 was calculated from the following equation: OVA-specific ^{51}Cr release = %^{51}Cr release from E.G7-OVA cells −%^{51}Cr release from EL4 cells. Each value represents the mean + S.D. (control group: n = 3, other groups: n = 5). Statistical analysis was performed by analysis of variance (**$P < 0.01$)

i.p. administration of Man-lipoplex induced a higher OVA-specific CTL response than local administration of naked pDNA. To demonstrate the antigen-specific anti-tumor effects induced by vaccination, E.G7-OVA cells (OVA expressing cells), and its parent cell line, pre-immunized mice were inoculated with EL4 cells (OVA non-expressing cells). Corresponding to the CTL response, the anti-tumor effects of the Man-lipoplex were observed only in E.G7-OVA cells and the effects of the Man-lipoplex were much greater than those following local administration of naked pDNA (Figure 6). These results suggest that the Man-lipoplex is an effective gene carrier for DNA vaccination used as cancer therapy.

To demonstrate mannose receptor-mediated gene transfection of the Man-lipoplex, its transfection characteristics in DCs were evaluated in both *in vitro* and *in vivo* experiments. As shown in Figures 1 and 2, the Man-lipoplex showed significantly higher uptake and transfection activity than the conventional lipoplex and this was reduced in the presence of mannan, a mannose receptor ligand. These *in vitro* results suggest that the Man-lipoplex is taken up by mannose receptor-mediated endocytosis by a dendritic cell line, DC2.4 cells. This observation is in good agreement with our previous report showing that the Man-lipoplex is taken up by mannose receptor-mediated endocytosis by primary cultured mouse peritoneal macrophages [22,32]. To evaluate the importance of mannose receptor-mediated gene transfection to DCs, we also evaluated the involvement of the mannose receptor-mediated mechanism in the CTL response. The

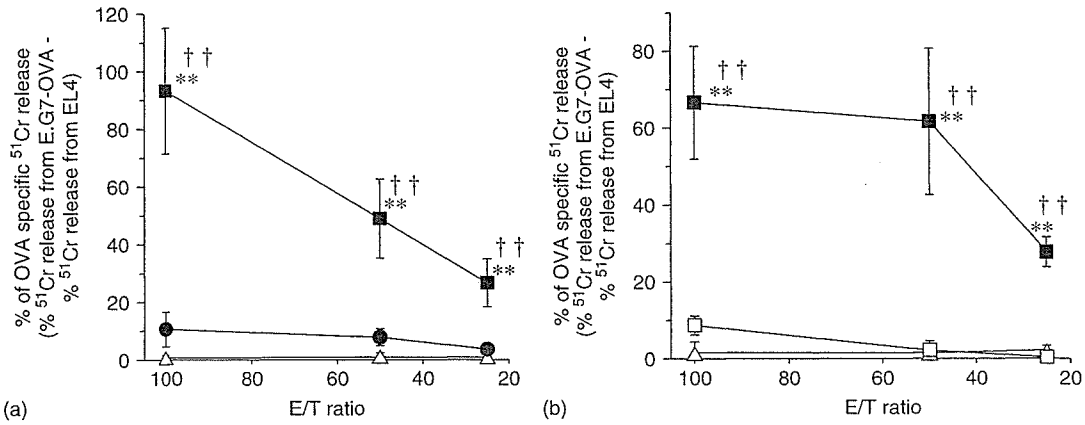

Figure 4. Effect of mannosylation of cationic liposomes on the induction of a CTL response. Mice were injected three times with naked pCMV-OVA (100 μg) or lipoplexes (pCMV-OVA; 100 μg) biweekly. (a) CTL response induced by the Man-lipoplexes (■) and the lipoplexes (●) or that of the no-treatment group (△). OVA-specific ^{51}Cr release was calculated from the following equation: OVA-specific ^{51}Cr release = %^{51}Cr release from E.G7-OVA cells −%^{51}Cr release from EL4 cells. Each value represents the mean ± S.D. (n = 4–5). (b) CTL response induced by the Man-lipoplex (■) or the Gal-lipoplex (□) or CTL response in the no-treatment group (△). OVA-specific ^{51}Cr release was calculated from the following equation: OVA-specific ^{51}Cr release = %^{51}Cr release from E.G7-OVA cells −%^{51}Cr release from EL4 cells. Each value represents the mean ± S.D. (n = 5). Statistical analysis was performed by analysis of variance. Significant difference between the no-treatment group (*$P < 0.05$, **$P < 0.01$) or pCMV-OVA given i.m. (††$P < 0.01$)

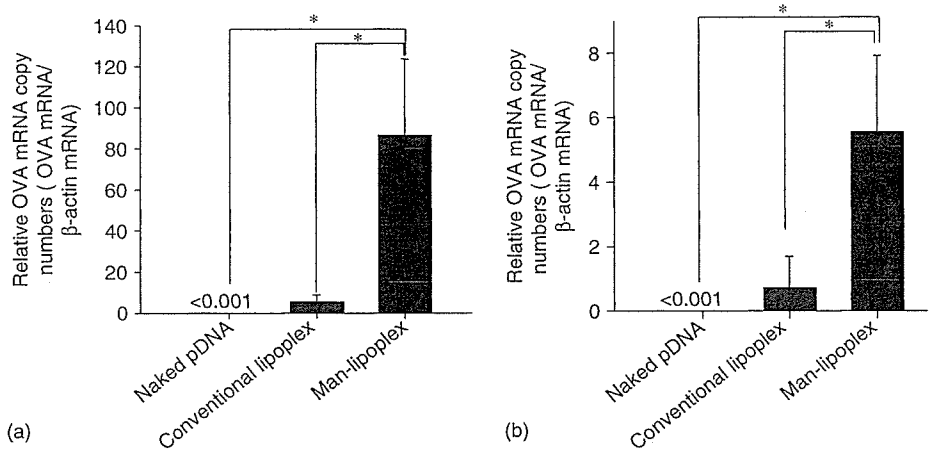

Figure 5. *In vivo* mRNA gene expression in CD11c$^+$ cells in the peritoneal cavity (a) and spleen (b) after i.p. administration to mice. Lipoplex or Man-lipoplex was prepared at a charge ratio (−/+) of 1.0 : 2.3 in 5% dextrose. Six hours after injection, OVA mRNA and β-actin mRNA eluted from CD11c$^+$ cells were measured by quantitative two-step RT-PCR. Each value represents the mean + S.D. (n = 3–4). Statistical analysis was performed by analysis of variance (*$P < 0.05$)

Gal-lipoplex was selected because it differed only from the Man-lipoplex by a sugar moiety. In a previous study, we have already confirmed that the Gal-lipoplex was taken up by asialoglycoprotein receptor-mediated endocytosis after intraportal administration [33,34]. As shown in Figure 4b, the CTL response of the Gal-lipoplex was significantly lower than that of the Man-lipoplex. These *in vitro* and *in vivo* results suggest that the Man-lipoplex is efficiently taken up by DCs via mannose receptor-mediated endocytosis.

As control cationic liposomes, cationic liposomes composed of 3β-[*N*,*N*′,*N*′-dimethylaminoethane]carbamoyl] cholesterol hydrochloride (DC-Chol liposomes) represent a feasible formulation for clinical trials involving gene therapy via the i.p. route [35] and it has also been reported that DC-Chol liposomes enhance DNA vaccine potency following i.p. administration in mice [36]. However, our preliminary experiment using pCMV-Luc demonstrated that DOTMA/Chol liposomes exhibited a much higher transfection activity than DC-Chol liposomes following i.p. administration (data not shown); therefore, DOTMA/Chol liposomes were selected as control liposomes for DNA vaccine therapy.

To further evaluate the effectiveness of lipoplex mannosylation, gene expression in APCs, OVA-specific CTL activity and the antitumor effect were compared with those obtained using conventional lipoplex. Since the lipid composition of the liposomes (DOTMA/Chol

DOI: 10.1002/jgm

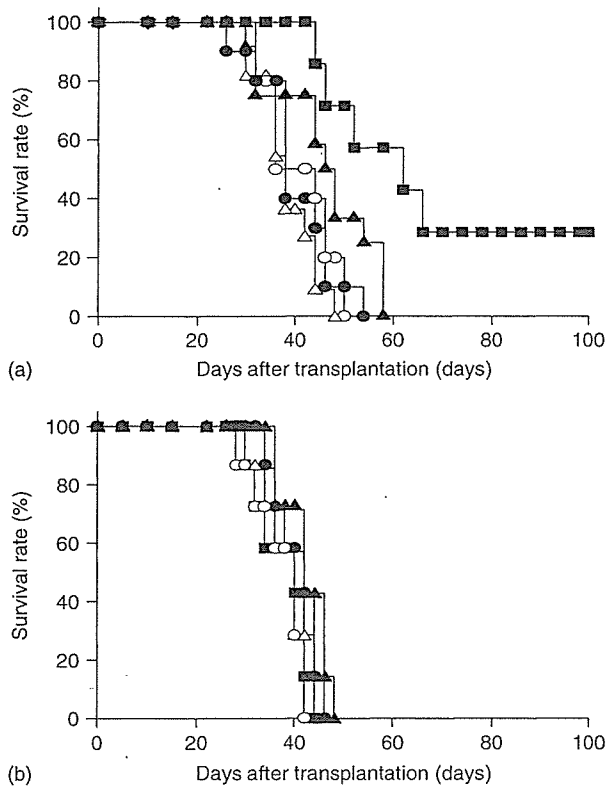

Figure 6. The anti-E.G7-OVA cell (a) or EL4 cell (b) tumor effect following pre-immunization by i.p. administration of various formulations or i.m. administration of naked pCMV-OVA solution (100 μg). Mice were injected with naked pCMV-OVA (○), the Man-lipoplex (■), or the lipoplex (●) given i.p., naked pCMV-OVA given i.m. (▲), or no treatment (△). E.G7-OVA (a) or EL4 (b) cells were transplanted into mice 2 weeks after the last immunization and the survival rate was determined (n = 7 for all groups in (b) and for Man-lipoplex in (a), n = 10 for all groups but the Man-lipoplex in (a))

vs. DOTMA/Chol/Man-C4-Chol) and the physicochemical properties (zeta-potential and particle size (see Results section)) of the lipoplex and Man-lipoplex are almost the same, the effect of mannosylation of lipoplex could be investigated by such comparisons. After i.p. administration of lipoplex or Man-lipoplex, the gene expression in $CD11c^+$ cells in the spleen and peritoneal cavity of Man-lipoplex was significantly higher than that of the conventional lipoplex (Figure 5a and 5b). Furthermore, the OVA-specific CTL response (Figure 4) and anti-tumor effect (Figure 6a) of the Man-lipoplex were significantly higher than that of the conventional lipoplex. These results convinced us that lipoplex mannosylation could enhance DNA vaccine potency.

As far as the effect of the administration route on the CTL activity by Man-lipoplex was concerned, the CTL activity following i.p. administration was higher than that following s.c. and i.m. administration (Figure 3a). We previously reported that the transfection efficiency of the lipoplex was lower than that of naked pDNA because the lipoplex is only localized at the injection site due to its cationic and macromolecular nature [37]. Thus, the lower CTL activity following s.c. and i.m. administration of the Man-lipoplex may be partly explained by our previous observation. In contrast, i.p. administrated Man-lipoplex is considered to reach the APCs in the peritoneal cavity and lymph nodes. Even the (large sized) cancer cells could distribute to the lymph nodes from the peritoneal cavity when undergoing metastasis [38,39]. Thus, these observations strongly suggest that i.p. administration is an effective administration route for gene transfection to APCs by the (Man-)lipoplex.

In the present study, we have demonstrated the effectiveness of i.p. administration of the Man-liposome formulation. This type of infusion of not only drugs such as cisplatin [42] and paclitaxel [43] but also cationic liposome/pDNA [44] has already been performed in clinical trials for ovarian cancer therapy. Regarding the i.p. administration method, implantable infusion pumps have been developed for a number of diseases [45] and there has been remarkable progress in endoscopic and laparoscopic surgical techniques [46]. These progresses in surgical techniques and devices might make i.p. administration of the Man-liposome formulation a conventional and feasible approach for the clinical application of DNA vaccine therapy.

In this study, we demonstrated that the Man-lipoplex enhanced gene expression via a mannose receptor-mediated mechanism. Since our previous study demonstrated that the Man-lipoplex were rapidly sorted from endosomes to lysosomes after uptake via mannose receptors [47], only a small part of pDNA seems to be released from endosome/lysosome to the cytosol and enters the nucleus for gene expression. Taking these findings into consideration, further modulation of intracellular sorting with some functional device should lead to more efficient gene expression in APCs. So far, functional materials such as influenza virus hemagglutinin subunit HA-2 (mHA2) [17], fusigenic peptide, and polyhistidine [48] have been grafted to the vectors to improve the intracellular sorting of cationic carrier/pDNA complexes. Modulation by grafting such functional molecules might be effective in the further development of the Man-lipoplex.

A large number of diseases can be potentially prevented or cured by DNA vaccination [40]. Recent developments in genomics technology have identified new target antigens, not only for infectious disease pathogens, but also for a large number of tumor-associated antigens [41] and this has increased the possibility of using DNA vaccines for a variety of infectious diseases and cancer therapies. Since the pDNA that encodes a variety of antigens has almost the same physicochemical properties as a polyanion, our Man-liposomes are expected to be applicable to a range of DNA vaccine therapies to enhance the CTL response.

In conclusion, we demonstrate that the Man-lipoplex produces an extremely high antigen-specific CTL response. In addition, intraperitoneal administration is an effective route for the APCs-selective gene transfection by the Man-lipoplex. Although further optimization

is required, this information will also be valuable for the future use, design, and development of a Man-lipoplex to enhance the potential of DNA vaccine therapy.

Acknowledgements

We are grateful to Dr. M. J. Bevan and Dr. K. L. Rock for providing us with pAc-neo-OVA and DC2.4 cells, respectively. This work was supported in part by Grants-in-Aid for Scientific Research from Ministry of Education, Culture, Sports, Science, and Technology of Japan, by Health and Labour Sciences Research Grants for Research on Advanced Medical Technology from the Ministry of Health, Labour and Welfare of Japan, by the Kao Foundation for Arts and Sciences, and by the Shimizu Foundation for the Promotion of Immunology Research.

References

1. Ulmer JB, Donnelly JJ, Parker SE, *et al.* Heterologous protection against influenza by injection of DNA encoding a viral protein. *Science* 1993; **259**: 1745–1749.
2. Schirmbeck R, Bohm W, Ando K, *et al.* Nucleic acid vaccination primes hepatitis B surface antigen specific cytotoxic T lymphocytes in non-responder mice. *J Virol* 1995; **69**: 5929–5934.
3. Donnelly JJ, Friedman A, Martinez D, *et al.* Preclinical efficacy of a prototype DNA vaccine: enhanced protection against antigenic drift in influenza virus. *Nat Med* 1995; **1**: 583–587.
4. Porgador A, Irvine KR, Iwasaki A, *et al.* Predominant role for directly transfected dendritic cells in antigen presentation to $CD8^+$ T cells after gene gun immunization. *J Exp Med* 1998; **188**: 1075–1082.
5. Akbari O, Panjwani N, Garcia S, *et al.* DNA vaccination: transfection and activation of dendritic cells as key events for immunity. *J Exp Med* 1999; **189**: 169–178.
6. Bot A, Stan AC, Inaba K, *et al.* Dendritic cells at a DNA vaccination site express the encoded influenza nucleoprotein and prime MHC class I-restricted cytolytic lymphocytes upon adoptive transfer. *Int Immunol* 2000; **12**: 825–832.
7. Mancini-Bourgine M, Fontaine H, Scott-Algara D, *et al.* Induction or expansion of T-cell responses by a hepatitis B DNA vaccine administered to chronic HBV carriers. *Hepatology* 2004; **40**: 874–882.
8. Rosenberg SA, Yang JC, Sherry RM, *et al.* Inability to immunize patients with metastatic melanoma using plasmid DNA encoding the gp100 melanoma-melanocyte antigen. *Hum Gene Ther* 2003; **14**: 709–714.
9. MacGregor RR, Ginsberg R, Ugen KE, *et al.* T-cell responses induced in normal volunteers immunized with a DNA-based vaccine containing HIV-1 env and rev. *AIDS* 2002; **16**: 2137–2143.
10. Arthur JF, Butterfield LH, Roth MD, *et al.* A comparison of gene transfer methods in human dendritic cells. *Cancer Gene Ther* 1997; **4**: 17–25.
11. Okada N, Tsukada Y, Nakagawa S, *et al.* Efficient gene delivery into dendritic cells by fiber-mutant adenovirus vectors. *Biochem Biophys Res Commun* 2001; **282**: 173–179.
12. Raper SE, Chirmule N, Lee FS, *et al.* Fatal systemic inflammatory response syndrome in a ornithine transcarbamylase deficient patient following adenoviral gene transfer. *Mol Genet Metab* 2003; **80**: 48–58.
13. Erbacher P, Bousser MT, Raimond J, *et al.* Gene transfer by DNA/glycosylated polylysine complexes into human blood monocyte-derived macrophages. *Hum Gene Ther* 1996; **7**: 721–729.
14. Kawakami S, Yamashita F, Nishida K, *et al.* Glycosylated cationic liposomes for cell-selective gene delivery. *Crit Rev Ther Drug Carrier Syst* 2002; **19**: 171–190.
15. Sudimack J, Lee RJ. Targeted drug delivery via the folate receptor. *Adv Drug Deliv Rev* 2000; **41**: 147–162.
16. Buning H, Ried MU, Perabo L, *et al.* Receptor targeting of adeno-associated virus vectors. *Gene Ther* 2003; **10**: 1142–1151.
17. Nishikawa M, Yamauchi M, Morimoto K, *et al.* Hepatocyte-targeted *in vivo* gene expression by intravenous injection of plasmid DNA complexed with synthetic multi-functional gene delivery system. *Gene Ther* 2000; **7**: 548–555.
18. Nishikawa M, Takemura S, Takakura Y, Hashida M. Targeted delivery of plasmid DNA to hepatocytes *in vivo*: optimization of the pharmacokinetics of plasmid DNA/galactosylated poly(L-lysine) complexes by controlling their physicochemical properties. *J Pharmacol Exp Ther* 1998; **287**: 408–415.
19. Kawakami S, Yamashita F, Nishikawa M, *et al.* Asialoglycoprotein receptor-mediated gene transfer using novel galactosylated cationic liposomes. *Biochem Biophys Res Commun* 1998; **252**: 78–83.
20. Morimoto K, Nishikawa M, Kawakami S, *et al.* Molecular weight-dependent gene transfection activity of unmodified and galactosylated polyethyleneimine on hepatoma cells and mouse liver. *Mol Ther* 2003; **7**: 254–261.
21. Nishikawa M, Takemura S, Yamashita F, *et al.* Pharmacokinetics and *in vivo* gene transfer of plasmid DNA complexed with mannosylated poly(L-lysine) in mice. *J Drug Target* 2000; **8**: 29–38.
22. Kawakami S, Sato A, Nishikawa M, *et al.* Mannose receptor-mediated gene transfer into macrophages using novel mannosylated cationic liposomes. *Gene Ther* 2000; **7**: 292–299.
23. Sato A, Kawakami S, Yamada M, *et al.* Enhanced gene transfection in macrophages using mannosylated cationic liposome-polyethylenimine-plasmid DNA complexes. *J Drug Target* 2001; **9**: 201–207.
24. Hattori Y, Kawakami S, Suzuki S, *et al.* Enhancement of immune responses by DNA vaccination through targeted gene delivery using mannosylated cationic liposome formulations following intravenous administration in mice. *Biochem Biophys Res Commun* 2004; **317**: 992–999.
25. Shen Z, Reznikoff G, Dranoff G., Rock KL. Cloned dendritic cells can present exogenous antigens on both MHC class I and class II molecules. *J Immunol* 1997; **158**: 2723–2730.
26. Cui Z, Han SJ, Huang L. Coating of mannan on LPD particles containing HPV E7 peptide significantly enhances immunity against HPV-positive tumor. *Pharm Res* 2004; **21**: 1018–1025.
27. Lee YC, Stowell CP, Krantz MJ. 2-Imino-2-methoxyethyl 1-thioglycosides: new reagents for attaching sugars to proteins. *Biochemistry* 1976; **15**: 3956–3963.
28. Moore MW, Carbone FR, Bevan MJ. Introduction of soluble protein into the class I pathway of antigen processing and presentation. *Cell* 1988; **54**: 777–785.
29. Kawakami S, Hattori Y, Lu Y, *et al.* Effect of cationic charge on receptor-mediated transfection using mannosylated cationic liposome/plasmid DNA complexes following the intravenous administration in mice. *Pharmazie* 2004; **59**: 405–408.
30. Kawakami S, Ito Y, Fumoto S, *et al.* Enhanced gene expression in lung by a stabilized lipoplex using sodium chloride for complex formation. *J Gene Med* 2005; **7**: 1526–1533.
31. Fumoto S, Kawakami S, Ito Y, *et al.* Enhanced hepatocyte-selective *in vivo* gene expression by stabilized galactosylated liposome/plasmid DNA complex using sodium chloride for complex formation. *Mol Ther* 2004; **10**: 719–729.
32. Hattori Y, Suzuki S, Kawakami S, *et al.* The role of dioleoylphosphatidylethanolamine (DOPE) in targeted gene delivery with mannosylated cationic liposomes via intravenous route. *J Control Release* 2005; **108**: 484–495.
33. Kawakami S, Fumoto S, Nishikawa M, *et al. In vivo* gene delivery to the liver using novel galactosylated cationic liposomes. *Pharm Res* 2000; **17**: 306–313.
34. Fumoto S, Nakadori F, Kawakami S, *et al.* Analysis of hepatic disposition of galactosylated cationic liposome/plasmid DNA complexes in perfused rat liver. *Pharm Res* 2003; **20**: 1452–1459.
35. Madhusudan S, Foster M, Muthuramalingam SR, *et al.* A multicenter phase I gene therapy clinical trial involving intraperitoneal administration of E1A-lipid complex in patients with recurrent epithelial ovarian cancer overexpressing HER-2/neu oncogene. *Clin Cancer Res* 2004; **10**: 2986–2996.
36. Ishii N, Fukushima J, Kaneko T, *et al.* Cationic liposomes are a strong adjuvant for a DNA vaccine of human immunodeficiency virus type 1. *AIDS Res Hum Retroviruses* 1997; **13**: 1421–1428.
37. Nomura T, Nakajima S, Kawabata K, *et al.* Intratumoral pharmacokinetics and *in vivo* gene expression of naked plasmid DNA and its cationic liposome complexes after direct gene transfer. *Cancer Res* 1997; **57**: 2681–2686.

38. Dubernard G, Morice P, Rey A, *et al.* Lymph node spread in stage III or IV primary peritoneal serous papillarycarcinoma. *Gynecol Oncol* 2005; 97: 136–141.
39. Dullens HF, Rademakers LH, Cluistra S, *et al.* Parathymic lymph nodes during growth and rejection of intraperitoneally inoculated tumor cells. *Invasion Metastasis* 1991; **11**: 216–226.
40. Donnelly JJ, Ulmer JB, Shiver JW, Liu MA. DNA vaccines. *Annu Rev Immunol* 1997; **15**: 617–648.
41. Polo JM, Dubensky TW Jr. Virus-based vectors for human vaccine applications. *Drug Discov Today* 2002; 7: 719–727.
42. Sabbatini P, Aghajanian C, Leitao M, *et al.* Intraperitoneal cisplatin with intraperitoneal gemcitabine in patients with epithelial ovarian cancer: results of a phase I/II trial. *Clin Cancer Res* 2004; **10**: 2962–2967.
43. Gelderblom H, Verweij J, van Zomeren DM, *et al.* Influence of Cremophor El on the bioavailability of intraperitoneal paclitaxel. *Clin Cancer Res* 2000; 8: 1237–1241.
44. Madhusudan S, Tamir A, Bates N, *et al.* A multicenter phase I gene therapy clinical trial involving intraperitoneal administration of E1A-lipid complex in patients with recurrent epithelial ovarian cancer overexpressing HER-2/neu oncogene. *Clin. Cancer Res* 2004; **10**: 2986–2996.
45. Hepp KD. Implantable insulin pumps and metabolic control. *Diabetologia* 1994; 37: S108–S111.
46. Stellato TA. History of laparoscopic surgery. *Surg Clin North Am* 1992; 72: 997–1002.
47. Yamada M, Nishikawa M, Kawakami S, *et al.* Tissue and intrahepatic distribution and subcellular localization of a mannosylated lipoplex after intravenous administration in mice. *J Control Release* 2004; 98: 157–167.
48. Midoux P, Kichler A, Boutin V, *et al.* Membrane permeabilization and efficient gene transfer by a peptide containing several histidines. *Bioconjugate Chem* 1998; 9: 260–267.

Effect of the Particle Size of Galactosylated Lipoplex on Hepatocyte-Selective Gene Transfection after Intraportal Administration

Yuriko HIGUCHI, Shigeru KAWAKAMI, Shintaro FUMOTO, Fumiyoshi YAMASHITA, and Mitsuru HASHIDA*

Department of Drug Delivery Research, Graduate School of Pharmaceutical Sciences, Kyoto University; Sakyo-ku, Kyoto 606–8501, Japan. Received March 20, 2006; accepted April 17, 2006; published online April 21, 2006

The purpose of this study was to examine the effect of the size of galactosylated cationic liposome (Gal-liposome)/plasmid DNA complex (Gal-lipoplex) on hepatocyte-selective gene transfection after intraportal administration. pCMV-Luc was selected as a model plasmid DNA. After intraportal administration of Gal-lipoplex to mice, the hepatic and intrahepatic gene expression was evaluated. To evaluate the effect of size, three different sizes of Gal-liposome were prepared. The mean particle sizes of Gal-lipoplex were about 141, 179, and 235 nm, respectively. The hepatic transfection efficacy was significantly enhanced by increasing the size of Gal-lipoplex. However, the gene expression in liver parenchymal cells (PC) of Gal-lipoplex of about 141 nm in size was significantly higher than that in liver non-parenchymal cells (NPC). In contrast, gene expression in PC of Gal-lipoplex of about 235 nm in size was significantly lower than that in NPC. These results highlight the importance of the Gal-lipoplex size for hepatocyte-selective gene transfer *in vivo*. The information in this study will be valuable for the future use, design, and development of Gal-lipoplex for *in vivo* applications.

Key words gene delivery; hepatocyte; targeting; galactosylated liposome; drug delivery system

Gene transfer to hepatocytes is of great therapeutic potential since hepatocytes are responsible for the synthesis of a wide variety of proteins that play important physiological roles. There has been much interest in *in vivo* gene transfer to the liver, as an alternate to *ex vivo* methods that require invasive surgery. So far, several methods involving the local administration of naked plasmid DNA (pDNA) has been tested in order to achieve gene delivery targeted to the liver.[1,2] Compared with these local applications to the liver, systemic application by vascular routes could transfect the gene to a large number of cells in the whole liver. However, the highest gene expression is observed in the lung after the intravenous[3—5] and intraportal[6] administration of cationic liposome/pDNA complex (lipoplex).

The development of targeted gene delivery systems is a promising approach for effective and safe *in vivo* gene transfer to hepatocytes. To achieve targeted gene delivery, galactose has been shown to be a promising targeting ligand for hepatocytes (liver parenchymal cells; PC) because these cells possess a large number of asialoglycoprotein receptors that recognize the galactose units on the synthetic galactosylated carriers.[7,8] Recently, we have developed Gal-liposomes containing cholesten-5-yloxy-*N*-(4-((1-imino-2-D-thiogalactosylethyl)amino)butyl) formamide (Gal-C4-Chol) for hepatocyte-selective gene transfection after intraportal administration to mice.[7,9,10] However, the level of *in vivo* gene expression was not as high as that expected from the *in vitro* results.[7,11] This phenomenon could explain the several barriers associated intrinsically with *in vivo* situations; therefore, these *in vivo* barriers need to be investigated to allow the successful development of an effective gene vector. However, little information is available about hepatocyte-selective gene transfer by Gal-lipoplex under *in vivo* conditions.

The passage through the sinusoids is considered an important factor for hepatocyte-selective gene transfection, since the Gal-lipoplex must pass through the endothelial cell barriers to reach the hepatocytes. In this study, therefore, we evaluated the effects of Gal-lipoplex size on hepatic transfection efficacy after intraportal administration. Once the *in vivo* gene expression is linked with its physicochemical properties including particle size, it is then possible to design a Gal-lipoplex to enable cell-specific *in vivo* gene delivery. *N*-[1-(2,3-Dioleyloxy)propyl]-*N*,*N*,*N*-trimethylammonium chloride (DOTMA)/cholesterol (Chol)/Gal-C4-Chol liposomes were selected as a Gal-liposome for study because of its hepatocyte-selectivity after intraportal administration.[7] pCMV-Luc was selected as a model pDNA for evaluating the gene expression by luciferase.

MATERIALS AND METHODS

Materials *N*-(4-Aminobutyl) carbamic acid *tert*-butyl ester and DOTMA were obtained from Tokyo Kasei Kogyo Co., Ltd. (Tokyo, Japan). Cholesterol (Chol) was obtained from Nacalai Tesque, Inc. (Kyoto, Japan). Cholesteryl chloroformate and collagenase type IA were obtained from Sigma Chemicals, Inc. (St. Louis, MO, U.S.A.). All other chemicals were of the highest purity available.

Animals Female five-week-old ICR mice (20—23 g) were purchased from the Shizuoka Agricultural Cooperative Association for Laboratory Animals (Shizuoka, Japan). All animal experiments were carried out in accordance with the Principles of Laboratory Animal Care as adopted and promulgated by the US National Institutes of Health and the Guidelines for Animal Experiments of Kyoto University.

Construction and Preparation of pDNA (pCMV-Luc) pCMV-Luc was constructed by subcloning the *Hin*dIII/*Xba*I firefly luciferase cDNA fragment from pGL3-control vector (Promega Co., Madison, WI, U.S.A.) into the polylinker of pcDNA3 vector (Invitrogen, Carlsbad, CA, U.S.A.). pDNA was amplified in the *E. coli* strain DH5a, isolated, and purified using a QIAGEN Endofree Plasmid Giga Kit (QIAGEN GmbH, Hilden, Germany). Purity was confirmed by 1% agarose gel electrophoresis followed by ethidium bromide staining and the pDNA concentration was measured by UV absorption at 260 nm.

Synthesis of Gal-C4-Chol Gal-C4-Chol was synthesized as reported previously.[11] Briefly, cholesteryl chlorofor-

* To whom correspondence should be addressed. e-mail: hashidam@pharm.kyoto-u.ac.jp

mate and *N*-(4-aminobutyl)carbamic acid *tert*-butyl ester were reacted in chloroform for 24 h at room temperature. A solution of trifluoroacetic acid and chloroform was added dropwise and the mixture was stirred for 4 h at 4 °C. The solvent was evaporated to obtain *N*-(4-aminobutyl)-(cholesten-5-yloxyl)formamide which was then combined with 2-imino-2-methoxyethyl-1-thiogalactoside and the mixture was stirred for 24 h at 37 °C. After evaporation, the resultant material was suspended in water, dialyzed against distilled water for 48 h (12 kDa cut-off dialysis tubing), and then lyophilized.

Preparation of Gal-liposome Gal-liposomes were prepared as reported previously.[7,10] The mixtures of DOTMA, Chol, and Gal-C4-Chol were dissolved in chloroform at a molar ratio of 2 : 1 : 1 for Gal-liposomes, vacuum-desiccated, and resuspended in sterile 5% dextrose solution at a concentration of 4 mg total lipids per ml. For small sized liposomes (about 49.6 nm, see Fig. 1), the suspension was sonicated for 3 min and the resulting liposomes were extruded 5-times through 100 nm polycarbonate membrane filters. In the case of medium (about 148 nm, see Fig. 1) and large (about 197 nm, see Fig. 1) sized liposomes, the resulting liposomes were directly extruded 5-times through 200 and 400 nm polycarbonate membrane filters, respectively.

Preparation of Gal-lipoplex Gal-lipoplex was prepared as reported previously.[7] pDNA in 5% dextrose solution was mixed with an equal volume of Gal-liposomes and incubated for 30 min. The mixing ratio of liposomes and pDNA was expressed as a charge ratio, which is the molar ratio of cationic lipids to pDNA phosphate residues.[12] As far as the charge ratio was concerned, we selected a charge ratio (−:+) of 1.0 : 2.3 for all experiments to obtain the most effective transfection activity for receptor-mediated gene transfer.[7] The particle size of the Gal-lipoplex was measured using a dynamic light scattering spectrophotometer (LS-900, Otsuka Electronics Co., Ltd., Osaka, Japan). The number-fractioned mean diameter was shown.

In Vivo* Transfection Experiments** Intraportal administration was performed as reported previously.[7,10] Mice were anesthetized by intraperitoneal administration of pentobarbital sodium (50 mg/kg), an incision was made in the abdomen, and the portal vein was exposed. The Gal-lipoplex was injected into the portal vein at a dose of 30 μg, and the abdomen was closed with wound clips. Liver samples were taken 6 h after injection and each sample was homogenized with lysis buffer (0.1 M Tris/HCl containing 0.05% Triton X-100 and 2 mM EDTA (pH 7.8)). After three cycles of freezing and thawing, the homogenates were centrifuged at 10000 ***g for 10 min at 4 °C. Twenty microliters of each supernatant was mixed with 100 ml; luciferase assay solution (Picagene, Toyo Ink Mfg. Co., Tokyo, Japan) and the light produced was immediately measured using a luminometer (Lumat LB 9507, Berthold Technologies, GmbH & Co., Bad Wildbad, Germany). The protein content of the samples was determined using a protein quantification kit (Dojindo Molecular Technologies, Inc., Gaithersburg, MD, U.S.A.). For evaluation of the intrahepatic localization of gene expression, the luciferase activities in the liver PC and non-parenchymal cells (NPC) were independently determined after centrifugal separation of PC and NPC in collagenase-digested liver as previously described.[7,9]

Statistical Analysis Statistical comparisons were performed by Student's *t*-test for two groups, Steel–Dwassl test for multiple groups.

RESULTS AND DISCUSSION

Recently, we developed Gal-C4-Chol with bi-functional properties of pDNA binding *via* electrostatic interaction and a high affinity for PC *via* their asialoglycoprotein receptors.[11] We have also demonstrated that the galactose density of Gal-liposomes is important for both effective recognition by asialoglycoprotein receptors and cell internalization *in vivo*.[13] Since Gal-C4-Chol possesses an imino group for binding to pDNA *via* electrostatic interaction, many galactose units could be introduce on the liposomal surface without loss of binding affinity to pDNA.[11] These promising properties of our Gal-lipoplex enable PC-selective gene transfer under *in vivo* conditions.[7,9,10]

In order to analyze the effect of Gal-lipoplex size, three different sizes of Gal-liposomes were prepared using extrusion method. Figure 1 shows the particle sizes of the Gal-liposomes and Gal-lipoplexes prepared. The mean particle sizes of Gal-liposomes prepared using 100, 200, and 400 nm polycarbonate filters were 49.6, 148, and 197 nm, respectively. The mean particle sizes of Gal-lipoplexes were 141, 179, and 235 nm, respectively. Using these Gal-lipoplexes with different particle sizes, the effect of Gal-lipoplex size on hepatic- and hepatocyte-selective gene transfection was stud-

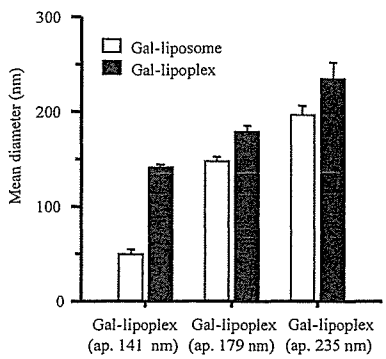

Fig. 1. The Particle Size Distribution of Gal-liposome and Gal-lipoplex

Each value represents the mean±S.D. of at least three experiments. ap.: approximately.

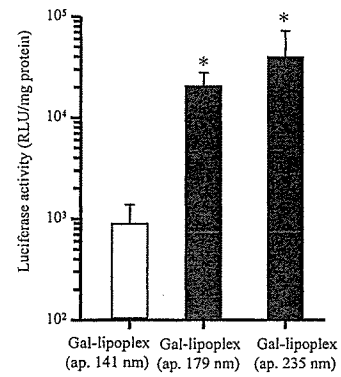

Fig. 2. Hepatic Transfection Activity of Gal-lipoplex after Intraportal Administration in Mice

Luciferase activity was determined 6 h post-injection of lipoplex. Statistically significant differences from galactosylated lipoplex (about 141 nm) (*$p<0.05$). Each value represents the mean±S.D. of at least three experiments. ap.: approximately.

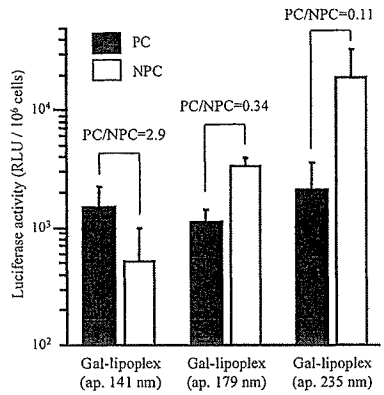

Fig. 3. Intrahepatic Transfection Activity of Gal-lipoplex after Intraportal Administration in Mice

Luciferase activity was determined 6h post-injection of lipoplex. Each value represents the mean±S.D. of at least three experiments. ap.: approximately.

ied.

We previously reported that gene expression in the liver was much higher than that in the lung, spleen, kidney, and heart after intraportal administration of Gal-lipoplex.[7] In the present study, the hepatic and intrahepatic gene expression characteristics were evaluated in relation to the size of Gal-lipoplex. As shown in Fig. 2, the hepatic transfection efficacy was significantly enhanced by an increase in the size of the Gal-lipoplex. To study the intrahepatic transfection activity, PC and NPC in the liver were separated by the collagenase perfusion technique (Fig. 3). The gene expression in PC of Gal-lipoplex about 141 nm in size was significantly higher than that in NPC. In contrast, the gene expression in PC of Gal-lipoplex about 179 and 235 nm in size was significantly lower than that in NPC. This finding might be due to the fact that the endothelial fenestrae measure 150—175 nm in diameter.[14]

Although we hypothesized that Gal-lipoplex over 200 nm in size has a limited ability to transfect the gene in liver because of the size limit, total hepatic gene expression was enhanced by increasing the size of the Gal-lipoplex (Fig. 2). This discrepancy may be partly explained by the presence of galactose particle receptors on Kupffer cells in NPC.[15] Kupffer cell would take up the Gal-lipoplex over 200 nm, which could not pass through the endothelial fenestrae. On the other hand, the uptake of the Gal-lipoplex over 200 nm by PC would be limited by the size of fenestrae. In fact, intrahepatic gene expression analysis demonstrated that Gal-lipoplex over 200 nm in size selectively transfect the gene in NPC (Fig. 3). These results highlight the importance of the Gal-lipoplex size for PC-selective gene transfer *in vivo*.

Physicochemical property of Gal-lipoplex is important concerning with PC-selective gene transfer *in vivo*.[16] Previously, we reported that the surface charge of Gal-lipoplex concerned with the interactions with blood components after intraportal injection of Gal-lipoplex[10] and charge of Gal-lipoplex affected on the gene expression.[7,17] In this study, it was revealed that the size of Gal-lipoplex had effect of the hepatic distribution of gene expression. However, Goncalves et al. reported that lipoplex with different size have different gravity, therefore, such factor also might contribute on the *in vivo* gene transfer of Gal-lipoplex.[18]

In conclusion, we prepared three different Gal-lipoplex about 141, 179, and 235 nm in size, and demonstrated that the hepatic transfection efficacy was enhanced by increasing the size of the Gal-lipoplex after intraportal administration. However, intrahepatic transfection was altered by the size of the Gal-lipoplex, *i.e.*, PC-selectivity by Gal-lipoplex about 141 nm in size; NPC-selectivity by Gal-lipoplex about 235 nm in size. The information described in this study will be valuable for the future use, design, and development of Gal-lipoplexes for *in vivo* applications.

Acknowledgements This work was supported in part by Grant-in-Aids for Scientific Research from Ministry of Education, Culture, Sports, Science, and Technology of Japan, and by Health and Labour Sciences Research Grants for Research on Advanced Medical Technology from the Ministry of Health, Labour and Welfare of Japan. The authors thank Kosuke Shigeta for technical assistance.

REFERENCES

1) Suzuki T., Shin B. C., Fujikura K., Matsuzaki T., Takata K., *FEBS Lett.*, **425**, 436—440 (1998).
2) Liu F., Huang L., *Gene Ther.*, **9**, 1116—1119 (2002).
3) Zhu N., Liggitt D., Liu Y., Debs R., *Science*, **261**, 209—211 (1993).
4) Uyechi L. S., Gagne L., Thurston G., Szoka F. C., Jr., *Gene Ther.*, **8**, 828—836 (2001).
5) Kawakami S., Ito Y., Fumoto S., Yamashita F., Hashida M., *J. Gene Med.*, **7**, 1526—1533 (2005).
6) Li S., Huang L., *Gene Ther.*, **4**, 891—900 (1997).
7) Kawakami S., Fumoto S., Nishikawa M., Yamashita F., Hashida M., *Pharm. Res.*, **17**, 306—313 (2000).
8) Hwang S. H., Hayashi K., Takayama K., Maitani Y., *Gene Ther.*, **8**, 1276—1280 (2001).
9) Fumoto S., Kawakami S., Ito Y., Shigeta K., Yamashita F., Hashida M., *Mol. Ther.*, **10**, 719—729 (2004).
10) Fumoto S., Kawakami S., Shigeta K., Higuchi Y., Yamashita F., Hashida M., *J. Pharmacol. Exp. Ther.*, **315**, 484—493 (2005).
11) Kawakami S., Yamashita F., Nishikawa M., Takakura Y., Hashida M., *Biochem. Biophys. Res. Commun.*, **252**, 78—83 (1998).
12) Yang J. P., Huang L., *Gene Ther.*, **4**, 950—960 (1997).
13) Managit C., Kawakami S., Yamashita F., Hashida M., *J. Pharm. Sci.*, **94**, 2266—2275 (2005).
14) Braet F., Wisse E., *Comp. Hepatol.*, **1**, 1—17 (2002).
15) Kolb-Bachofen V., Schlepper-Schafer J., Vogell W., Kolb H., *Cell*, **29**, 859—866 (1982).
16) Kawakami S., Yamashita F., Nishida K., Nakamura J., Hashida M., *Crit. Rev. Ther. Drug Carrier Syst.*, **19**, 171—190 (2002).
17) Fumoto S., Nakadori F., Kawakami S., Nishikawa M., Yamashita F., Hashida M., *Pharm. Res.*, **20**, 1452—1459 (2003).
18) Goncalves E., Debs R. J., Health T. D., *Biophys. J.*, **86**, 1554—1563 (2004).

Available online at www.sciencedirect.com
ScienceDirect
Journal of Controlled Release 114 (2006) 193–201
journal of controlled release
www.elsevier.com/locate/jconrel

Effect of mannose density on mannose receptor-mediated cellular uptake of mannosylated O/W emulsions by macrophages

Wassana Yeeprae, Shigeru Kawakami, Fumiyoshi Yamashita, Mitsuru Hashida *

Department of Drug Delivery Research, Graduate School of Pharmaceutical Sciences, Kyoto University, Sakyo-ku, Kyoto 606-8501, Japan

Received 14 February 2006; accepted 11 April 2006
Available online 9 May 2006

Abstract

Carbohydrate grafted emulsions are one of the most promising cell-specific targeting systems for lipophilic drugs. We have previously reported that mannosylated (Man-) emulsions composed of soybean oil, EggPC and cholesten-5-yloxy-*N*-(4-((1-imino-2-D-thiomannosylethyl)amino) alkyl)formamide (Man-C4-Chol) with a ratio of 70:25:5 were significantly delivered to liver non-parenchymal cells (NPC) via mannose receptor-mediated mechanism after intravenous administration in mice. Since the efficient targeting through a receptor-mediated mechanism is largely controlled by ligand–receptor interaction, the effect of mannose density on Man-emulsions was studied with regard to both the disposition in vivo in mice and the uptake in vitro, using elicited macrophages which express a number of mannose receptors. After intravenous injection, Man-emulsions with 5.0% (Man-5.0-emulsions) and 7.5% (Man-7.5-emulsions) of Man-C4-Chol were rapidly eliminated from the blood circulation and preferentially accumulated in the liver-NPC compared with Man-emulsions with 2.5% of Man-C4-Chol (Man-2.5-emulsions) and bare emulsions (Bare-emulsions). The in vitro study showed increased internalization of Man-5.0- and Man-7.5-emulsions and significant inhibition of uptake in the presence of mannan. The enhanced uptake of Man-emulsions was related to the increasing of Man-C4-Chol content that corresponded to confocal microscopy study. These results suggest that the mannose density of Man-emulsions plays an important role in both cellular recognition and internalization via a mannose receptor-mediated mechanism.

Keywords: Mannosylated emulsion; Macrophage; Mannose receptor; Mannose density; Targeting; Uptake

1. Introduction

Macrophages play a pivotal role in health and a variety of diseases such as innate and adaptive immunity [1], inflammation [2], Gaucher's disease [3] and tuberculosis [4]. A number of suitable strategies have been developed for macrophage-selective targeting systems [5]. Among them, receptor-mediated drug and gene targeting is one of the most promising approaches to achieve efficient therapy and minimize systemic toxicity [6]. One particular strategy involves the sugar recognition mechanism whereby receptors can recognize the corresponding sugars on the non-reducing terminal of sugar chains thereby mediating cellular uptake [7]. Of particular interest are mannose receptors, a 175 kDa transmembrane protein of the C-type lectin family [8], containing multiple C-type lectin domains (CTLDs) [9], which are present on the surface of macrophages and capable of recognizing and internalizing mannose, fucose and *N*-acetylglucosamine terminated molecules [10,11].

However, the success of macrophage-selective delivery systems crucially depends on the ability to deliver drugs or agents to the intracellular site for the desired pharmacological action. Inadequate specificity for macrophages and poor internalization of drug-carrier conjugates are critical obstacles to their success. It is known that the efficiency of ligand recognition depends on the ligand–receptor interaction, multivalent ligands with a "cluster effect" showed higher binding affinity to their counter receptors than monovalent ligand [12–14]. Nevertheless, we have previously demonstrated the selective delivery of liposomes [15,16] and plasmid DNA/liposome complexes [17,18] modified with novel mannosylated cholesterol derivatives, cholesten-5-yloxy-*N*-(4-((1-imino-2-D-thiomannosylethyl)amino)butyl)

* Corresponding author. Tel.: +81 75 753 4525; fax: +81 75 753 4575.
E-mail address: hashidam@pharm.kyoto-u.ac.jp (M. Hashida).

0168-3659/$ - see front matter © 2006 Published by Elsevier B.V.
doi:10.1016/j.jconrel.2006.04.010

formamide (Man-C4-Chol), as a monovalent ligand to mannose receptors.

As far as lipophilic drug delivery systems are concerned, lipid emulsions are more appropriate than other carrier systems due to their physical stability, biocompatibility and highly solubilizing capacity [19,20]. We have previously reported the in vivo disposition of mannosylated emulsions (Man-emulsions) after intravenous administration in mice [21]. Man-emulsions were rapidly and mainly delivered to the liver and exhibited a high hepatic uptake clearance; nearly equal to the hepatic blood flow rate, within 10 min and were predominantly recovered in liver non-parenchymal cells (NPC) with a high NPC/parenchymal cell (PC) ratio. These results confirmed that the hepatic uptake of Man-emulsions was via mannose receptor-mediated uptake and suggested that Man-emulsions are a promising carrier for NPC targeting. We have previously demonstrated that one of the most important factors for recognition by mannose receptors is the mannose density of mannosylated proteins [22]. These observations prompted us to investigate the effect of mannose density on the uptake of Man-emulsions via mannose receptor-mediated uptake in order to achieve a more rational approach to the design of drug delivery systems.

Although in vivo uptake experiments have confirmed the uptake of Man-emulsions via a mannose receptor-mediated mechanism, this uptake mechanism could not be defined clearly because of complications in the in vivo study including interaction with endogenous substances [23,24], multispecificity of ligand recognition [10,11] and differences in the cellular localization of mannose receptors [25].

To examine the effect of the mannose density on the surface of Man-emulsions for efficient targeting to macrophages, Man-emulsions with different ratios of Man-C4-Chol were characterized in a series of in vivo and in vitro studies. The in vivo and in vitro experiments with Man-emulsions showed enhanced uptake of Man-emulsions with increasing mannose density. These results demonstrate the influence of the mannose density of Man-emulsions on their recognition and internalization by mannose receptors.

2. Materials and methods

2.1. Materials

Soybean oil was supplied from Wako Pure Chemicals Industry, Ltd. (Osaka, Japan). Egg phosphatidylcholine (EggPC) was purchased from Avanti Polar Lipids, Inc. (Alabaster, AL, USA). Cholesteryl chloroformate and pyridine were purchased from Sigma-Aldrich, Co. (St. Louis, MO, USA). [^{3}H]Cholesteryl hexadecyl ether (CHE) was supplied by NEN Life Science Products Inc. (Boston, MA, USA) and *N*-(4-aminobutyl)carbamic acid *tert*-butyl ester was obtained from Tokyo Kasei Kogyo Co., Ltd. (Tokyo, Japan). Cholesterol (Chol), mannan from *yeast extract* and iodoacetate were purchased from Nacalai Tesque, Inc. (Kyoto, Japan). Soluene-350 was obtained from Packard Co., Inc. (Groningen, The Netherlands). Other chemicals used were of the highest purity available.

2.2. Synthesis of Man-C4-Chol

Man-C4-Chol was synthesized by the method described previously [15]. Briefly, cholesteryl chloroformate was reacted with *N*-(4-aminobutyl)carbamic acid *tert*-butyl ester in chloroform for 24 h at room temperature and then incubated with trifluoroacetic acid for 4 h at 4 °C. *N*-(4-Aminobutyl)-(cholesten-5-yloxyl)formamide was obtained after evaporation. A quantity of the resulting material was added to an excess of 2-imino-2-methoxyethyl-1-thio-mannoside [26] in pyridine containing triethylamine. After 24 h incubation at room temperature, the reaction mixture was evaporated, resuspended in water and dialyzed against distilled water for 48 h using a dialysis membrane (12 kDa cutoff), and finally lyophilized.

2.3. Preparation of O/W emulsions

Emulsions were prepared by the method described previously [20]. Bare- or Man-emulsions consisting of soybean oil, EggPC, and Chol or Man-C4-Chol at various weight ratios were used. The lipid mixtures with a trace amount of [^{3}H]CHE were dissolved in chloroform. For confocal microscopy study, fluorescent phosphatidylethanolamine (PE)–carboxyfluorescein (1 mol%) was added to the chloroform mixture. The dried film was then vacuum-desiccated and resuspended in pH 7.4 phosphate buffered saline (PBS). The suspensions were sonicated for 1 h (200 W) under a current of nitrogen. The particle sizes and zeta potentials of the emulsions were determined using a Zetasizer Nano ZS instrument (Malvern Instruments, Ltd., Worcestershire, UK). The concentration of the emulsions was adjusted to suitable concentrations based on the radioactivity of the [^{3}H]CHE-labeled emulsions.

2.4. Animals

Four- to five-week-old male ddY and ICR mice were obtained from the Shizuoka Agriculture Cooperative Association for Laboratory Animals (Shizuoka, Japan). All animal experiments were carried out in accordance with the Principles of Laboratory Animal Care as adopted and propagated by the US National Institutes of Health and the Guideline for Animal Experiments of Kyoto University.

2.5. In vivo distribution study

[^{3}H]CHE (0.1 μCi/100 μL)-labeled emulsions at a lipid concentration of 0.5% were injected into the tail vein of male ddY mice at a dose of 25 mg/kg. At given times, mice were sacrificed, and then blood samples from the vena cava, liver, spleen, heart, lung, kidney, muscle and urine were collected and dissolved in Soluene-350 for radioactivity measurement using a liquid scintillation counter LSC6100 (Aloka Inc., Tokyo, Japan).

2.6. Determination of tissue uptake clearances of emulsions

Tissue distribution data were evaluated using the organ distribution clearances as reported previously [27]. Briefly,

the tissue uptake rate can be described by the following equation:

$$\frac{dX_t}{dt} = CL_{uptake} \cdot C_b \quad (1)$$

where X_t is the amount of [^{3}H]CHE-labeled emulsions in the tissue at time t, CL_{uptake} is the tissue uptake clearance and C_b is the blood concentration of [^{3}H]CHE-labeled emulsions. Integration of Eq. (1) gives

$$X_t = CL_{uptake} \cdot AUC_{(0-t)} \quad (2)$$

where $AUC_{(0-t)}$ represents the area under the blood concentration–time curve from time 0 to t. The CL_{uptake} value can be obtained from the initial slope of a plot of the amount of [^{3}H]CHE-labeled emulsion in the tissue at time t (X_t) vs. the area under the blood concentration–time curve from time 0 to t [$AUC_{(0-t)}$].

2.7. Hepatic cellular localization of emulsions

The separation of liver-PC and NPC was performed by the collagenase perfusion method [28,29]. Briefly, mice were anesthetized with pentobarbital (40–60 mg/kg) after an intravenous injection of with 0.5% [^{3}H]CHE (0.5 μCi/100 μL)-labeled emulsions at a dose 25 mg/kg. Thirty minutes later, the liver was perfused via the portal vein with perfusion medium (Ca^{2+},Mg^{2+}-free HEPES solution, pH 7.2) for 10 min and then with HEPES solution containing 5 mM $CaCl_2$ and 0.05% (w/v) collagenase (type I) solution at pH 7.5 for 10 min. As soon as the perfusion started, the vena cava and aorta were cut and the perfusion rate was maintained at 3–4 mL/min. Following the discontinuation of perfusion, the liver was excised and its capsular membranes were removed. The cells were suspended by gentle stirring in ice-cold Hank's-HEPES buffer containing 0.1% bovine serum albumin (BSA). The dispersed cells were filtered through gauze and centrifuged at 50×g for 1 min. The pellets (PC-enriched fraction) and the supernatant (NPC-enriched fraction) were subjected to repeated low-speed differential centrifugation for cell purification [30,31]. The pellets containing the liver-PC were washed twice with Hank's-HEPES solution and then centrifuged at 50×g for 1 min for three times. The supernatant containing liver-NPC was similarly centrifuged until there was no cell pellet contamination. The resulting material was then centrifuged twice at 200×g for 2 min and then at 400×g for 2 min. PC and NPC were resuspended separately in ice-cold Hank's-HEPES solution (4 mL for PC and 2 mL for NPC). The number of viable cells was determined by the trypan blue exclusion method. Then, the radioactivity in the cells (0.5 mL) was measured using a liquid scintillation counter LSC6100 (Aloka Inc., Tokyo, Japan).

2.8. Harvesting and culture of macrophages

Elicited macrophages were harvested from the peritoneal cavity of male ICR mice 4 days after intraperitoneal injection of 1 mL 2.9% thioglycolate medium (Nissui Pharmaceutical, Tokyo, Japan). Cells were washed, then suspended in RPMI 1640 supplemented with 10% heat-inactivated fetal bovine serum (MP Biomedical Inc., OH, USA), penicillin G (100 U/mL) and streptomycin (100 μg/mL). The cells were plated on 12-well Falcon® culture plates (Becton Dickinson Labware Inc., Franklin Lakes, NJ, USA) at a density of 1.3×10^5 cells/cm^2. After incubation for 6 h at 37 °C in 5% CO_2–95% O_2, non-adherent macrophages were washed off with culture medium and then cultured under the same conditions.

2.9. In vitro uptake study

Uptake experiments were carried out after 72 h cultivation [32]. Cells were washed twice with 1 mL pH 7.4 Hank's balanced salt solution (HBSS), then cultured with [^{3}H]CHE-labeled emulsions at concentration of 0.12 mg/mL (0.06 μCi/mL). For the inhibition study, macrophages were incubated with the mixture of emulsions and inhibitors or pre-incubated with 1 mM of iodoacetate, endocytotic inhibition, for 30 min prior to emulsions [33]. After incubation at 4 or 37 °C, the cells were washed five times with ice-cold PBS buffer. For the internalization study, the cells were washed five times with ice-cold acetate buffer pH 4.0 or 20 mM EDTA in PBS buffer to remove the emulsions bound to the cell surface. The cells were then solubilized in 0.5 mL 1 M NaOH overnight and neutralized with 0.1 mL 5 M HCl. The radioactivity was measured using a liquid scintillation counter LS2500 (Beckman Coulter, Inc., Tokyo, Japan). The protein content was determined by a Proteostain Protein Quantification Kit (Doiindo Molecular Technologies, Inc., MD, USA). The radioactivity was normalized with respect to the protein content of the cells.

2.10. Confocal microscopy study

The isolated macrophages were cultured at a density of 1.3×10^5 cells/cm^2 on a glass-bottom 12-well plate. After a 72 h cultivation, the cells were washed twice with 1 mL HBSS, and then incubated at 4 or 37 °C with 0.12 mg/mL of PE-carboxyfluorescein emulsions. After a 2 h incubation, the cells were washed five times with ice-cold HBSS, then fixed with 4% paraformaldehyde and 0.01% glutaraldehyde in PBS (+) for 10 min on ice and washed three times with ice-cold HBSS. For plasma membrane staining, fixed cells were incubated with 20 μg/mL rhodamine–concanavalin A (ConA) at room temperature for 5 min [34]. After washing twice with 1 mL ice-cold HBSS, cover glasses were mounted on slide glasses with 50% glycerol–2.5% DABCO (1,4-diazabicyclo-[2,2,2] octane) (Sigma Chemical Co., Inc., St. Louis, MO, USA) in PBS. The samples were examined by a Fluoview® confocal laser microscope (Olympus Inc., Tokyo, Japan). The objective specifications were 40× oil immersion and numerical aperture 1.0.

2.11. Statistical analysis

Statistic analysis was performed using Student's paired t-test for two groups and the Turkey–Kramer test for multiple

comparisons between groups. $P<0.05$ was considered to be indicative of statistical significance.

3. Results

3.1. Physicochemical properties of emulsions

The lipid composition, mean particle sizes and zeta potentials of the emulsions are shown in Table 1. Among the various ratios of Man-C4-Chol containing emulsions, the mean particle sizes were about 75–90 nm, whereas the zeta potentials were slightly increased in accordance with the content ratio of Man-C4-Chol. However, there was no significant difference in physicochemical properties among these emulsions.

3.2. In vivo distribution study and pharmacokinetic analysis

To determine the influence of mannose density on the in vivo disposition of Man-emulsions, mice were intravenously injected with 0.5% [^{3}H]CHE-labeled emulsions, and then the radioactivity in blood and tissue samples was measured versus time. Bare- and Man-emulsions were rapidly eliminated from the blood circulation (Fig. 1A) and predominately recovered in the liver within the first 10 min (Fig. 1B). Man-5.0- and Man-7.5-emulsions exhibited significant accumulation in the liver, accounting for 70% and 80% of the dose, respectively. In contrast, Man-2.5-emulsions had a similar liver accumulation, about 50% of the dose, to that of Bare-emulsions.

The tissue uptake clearance was analyzed in the early phase up to 10 min to avoid the tissue uptake efflux of [^{3}H]CHE. Table 2 summarizes the pharmacokinetic parameters including the AUC and the uptake clearances of Bare- and Man-emulsions. The uptake clearances were determined for liver (CL_{liver}), spleen (CL_{spleen}), heart (CL_{heart}), lung (CL_{lung}), kidney (CL_{kidney}), muscle (CL_{muscle}) and urine (CL_{urine}). This pharmacokinetic analysis provided information about the uptake clearance characteristics of these emulsions with a small AUC and a large hepatic uptake clearance. Although their hepatic uptake clearance was the highest among the tissues examined, the hepatic uptake clearances of Man-5.0- and Man-7.5-emulsions were similarly high and about 3.5 times greater than those of Bare- and Man-2.5-emulsions. Bare- and Man-2.5-emulsions had identical AUC and hepatic uptake clearance values.

Table 1
The lipid composition, mean particle sizes and zeta potentials of emulsions

Emulsions (lipid composition, weight ratio)	Mean particle size (nm)	Zeta potential (mV)
Bare-emulsions (soybean oil/EggPC/Chol, 70:25:5.0)	85±5.1	−1.1±1.5
Man-2.5-emulsions (soybean oil/EggPC/Man-C4-Chol, 70:27.5:2.5)	90±13	−0.2±0.3
Man-5.0-emulsions (soybean oil/EggPC/Man-C4-Chol, 70:25:5.0)	75±3.0	2.2±3.4
Man-7.5-emulsions (soybean oil/EggPC/Man-C4-Chol, 70:22.5:7.5)	80±1.7	7.4±3.0

Each value represents the mean±S.D. values ($n=3$).

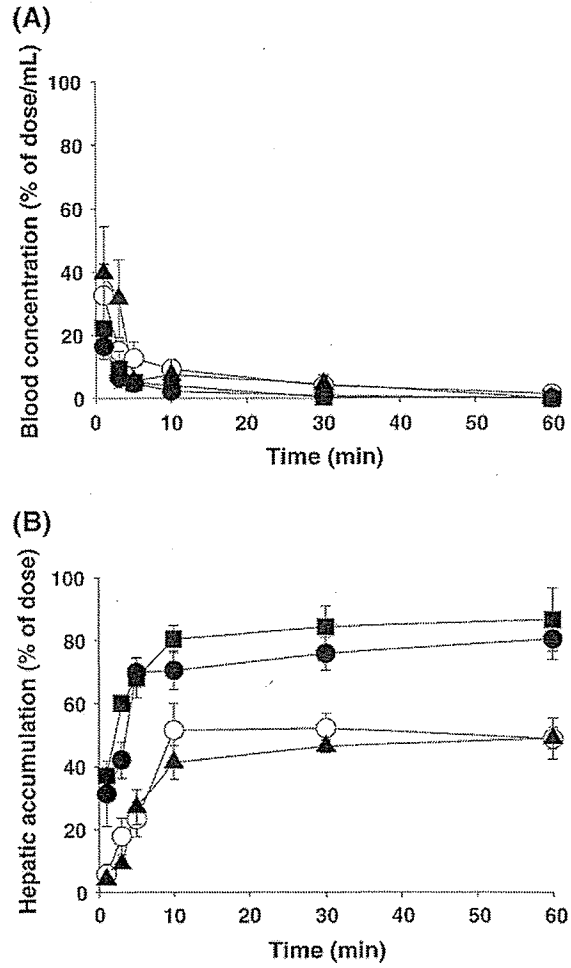

Fig. 1. (A) Blood concentration and (B) hepatic accumulation of Bare- (○), Man-2.5- (▲), Man-5.0- (●) and Man-7.5- (■) emulsions following intravenous injection in mice. Each value represents the mean±S.D. of three experiments.

3.3. Hepatic cellular localization

To examine the cell-selective targeting ability of Man-emulsions, the hepatic cellular distribution of 0.5% [^{3}H]CHE-labeled emulsions 30 min post-administration was studied by the collagenase method (Fig. 2). The distribution in NPC and PC was determined by the NPC/PC ratio after normalization of cell numbers. The affinity of these emulsions for NPC was increased in parallel with the Man-C4-Chol content. Man-5.0 and Man-7.5-emulsions were clearly preferentially localized in NPC with a high NPC/PC ratio, 2.0 and 13.7, respectively ($P<0.001$) with a similar degree of uptake. However, Man-2.5-emulsions were equally localized in NPC and PC, whereas Bare-emulsions were predominately localized in PC with a low NPC/PC ratio, 0.4 ($P<0.05$).

Table 2
Area under the blood concentration–time curve (AUC) and tissue uptake clearance of [^{3}H]CHE-labeled emulsions after intravenous injection into mice[a]

Emulsions	AUC[a]	Tissue uptake clearance (μL/h)						
	(% of dose h/mL)	CL_{liver}	CL_{spleen}	CL_{heart}	CL_{lung}	CL_{kidney}	CL_{muscle}	CL_{urine}
Bare-emulsions	2.8	18,300	724	1067	161	129	26	12
Man-2.5-emulsions	2.8	14,800	390	2060	145	140	32	15
Man-5.0-emulsions	1.2	60,500	4493	699	621	138	13	12
Man-7.5-emulsions	1.4	56,000	3521	272	1086	716	–	56

[a] The AUC and tissue uptake clearances were calculated for periods up to 10 min after intravenous injection. An average of three experiments is shown.

3.4. In vitro uptake study

In order to define the uptake characteristics of Man-emulsions, the uptake conditions were studied in terms of the dose, temperature and incubation time. Fig. 3A shows the dose-dependent in vitro uptake of Bare- and Man-5.0-emulsions by elicited macrophages at 37 °C for 2 h. The uptake of Man-5.0-emulsions markedly depended on the dose compared with that of Bare-emulsions. The uptake time courses both at 4 and 37 °C are shown in Fig. 3B. Man-5.0-emulsions were increasingly taken up over the incubation time at 37 °C compared with Bare-emulsions ($P<0.01$), although the uptake of both Man-5.0- and Bare-emulsions was very low at 4 °C.

3.5. Uptake inhibition study

To verify the uptake mechanism of Man-emulsions in a mannose receptor-mediated manner, competitive uptake experiments on [^{3}H]CHE-labeled emulsions were performed with or without an excess of mannan, a known ligand for mannose receptors, and unlabeled bare-emulsions (Fig. 4). The highest cellular uptake was observed in Man-7.5-emulsions, followed by Man-5.0-emulsions, Man-2.5-emulsions and uptake was considerably lower by Bare-emulsions. The uptake by Man-emulsions with different Man-C4-Chol ratios was significantly inhibited in the presence of 1 mg/mL mannan ($P<0.05$ and 0.01) but not by bare-emulsions. On the other hand, the uptake of Bare-emulsions was markedly suppressed by only co-incubation with bare-emulsions ($P<0.01$).

To confirm whether mannose residues trigger the binding and internalization of Man-emulsions into macrophages, the amount of surface binding and internalization of emulsions in macrophages were determined by pre-incubation with 1 mM

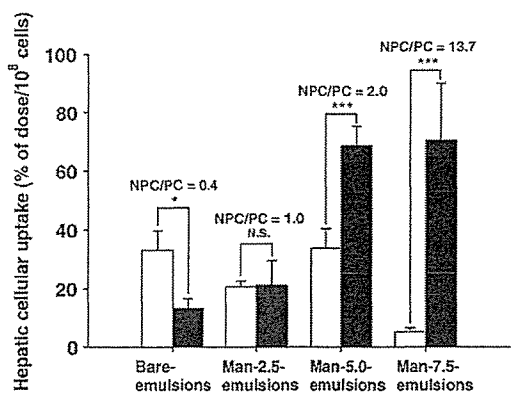

Fig. 2. Hepatic cellular localization of emulsions after intravenous injection in mice. Radioactivity was determined 30 min post-injection in PC (□) and NPC (■). Each value represents the mean±S.D. of three experiments. Statistically significant differences (*$P<0.05$, ***$P<0.001$) between PC and NPC in each group; N.S., not significant.

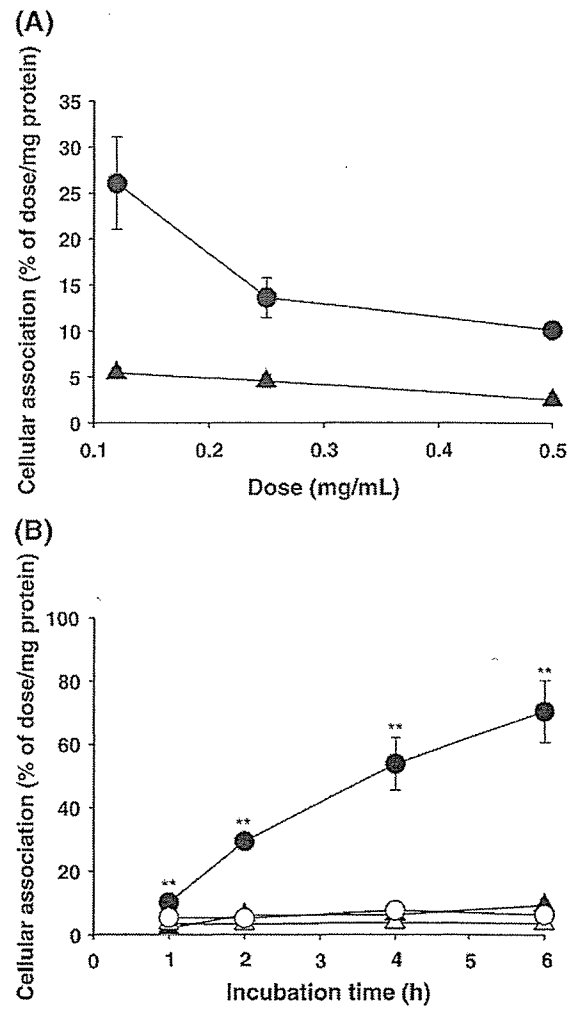

Fig. 3. (A) Dose-dependent cellular uptake of Bare-emulsions (▲) and Man-5.0-emulsions (●). Elicited macrophages were incubated with different concentrations of emulsions at 37 °C for 2 h. (B) The uptake time-course of 0.12 mg/mL of Bare-emulsions (▲, △) and Man-5-emulsions (●, ○) at 4 (opened) or 37 °C (filled) for given incubation time. Results are expressed the mean±S.D. of three experiments. Statistically significant differences (**$P<0.01$) from Bare-emulsions at each time point.

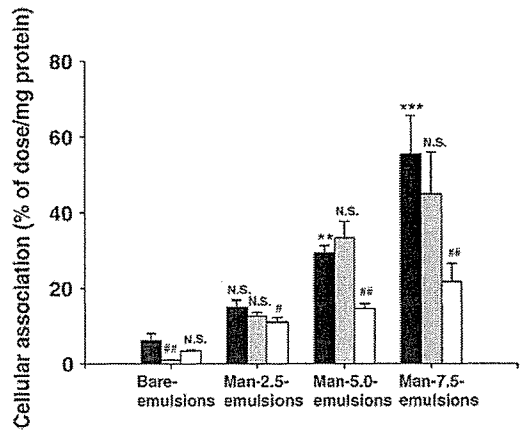

Fig. 4. The uptake of 0.12 mg/mL of emulsions by elicited macrophages. Macrophages were incubated with each emulsions alone (black) or with 1 mg/mL of bare-emulsions (grey) or 1 mg/mL of mannan (white). The amount of emulsions associated with the cells was measured following a 2 h incubation at 37 °C. Each value represents the mean±S.D. of three experiments. Statistically significant differences (**$P<0.01$, ***$P<0.001$) from control of Bare-emulsions (#$P<0.05$, ##$P<0.01$) from control of each group; N.S., not significant.

iodoacetate and washing with acetate buffer pH 4 or 20 mM EDTA in PBS, respectively (Fig. 5). Since the binding of mannose residues to mannose receptors has been reported to be sensitive to the environmental pH and calcium ions [35,36], these methods could be applied to determine the amount of internalized Man-emulsions. The amount of surface-bound and internalized emulsions obtained by these different methods was identical. Bare-emulsions underwent hardly any binding to the surface of macrophages, and then were internalized into the cells to a minor extent. Although Man-2.5-emulsions were bound to the cell surface to some extent, they underwent scarcely any internalization into the cells. In contrast, Man-5.0-($P<0.01$) and Man-7.5-emulsions ($P<0.001$) showed a significantly increase in surface binding and exhibited extensive uptake into the cells compared with Bare-emulsions. The uptake amount was reduced when cells were pretreated with iodoacetate. These inhibition studies also demonstrated the influence of acid and ions on the binding and internalization of Man-emulsions.

3.6. Confocal microscopy study

The cellular association of fluorescent emulsions after a 2 h incubation at 4 and 37 °C is shown in Fig. 6. Confocal microscopy images revealed a temperature-dependent binding (4 °C) and internalization (37 °C) of emulsions. In addition, the surface binding and internalization of Man-emulsions were increased with regard to the Man-C4-Chol content in a manner similar to that found in the in vitro uptake experiments.

4. Discussion

The internalization of drug-carrier conjugates into target cells is an important method of obtaining therapeutic efficacy. In order to evaluate the influence of the mannose density on the internalization of Man-emulsions in vivo, mice were intravenously injected with Man-emulsions containing different ratios of Man-C4-Chol. After intravenous administration, Man-5.0- and Man-7.5-emulsions were largely taken up by the liver (Fig. 1) accompanied by a high hepatic uptake clearance (Table 2) that was nearly equal to the hepatic plasma flow rate (66,000 μL/h) [37]. Furthermore, Man-5.0- and Man-7.5-emulsions selectively distributed into NPC, rather than PC, with high NPC/PC ratio (based on cell number) compared with Bare- and Man-2.5-emulsions (Fig. 2). However, the whole liver uptake of Man-7.5-emulsions was predominantly contributed by NPC, whereas that of Man-5.0-emulsions was equally involved by NPC and PC. These results indicate that Man-emulsions exhibit efficient and selective targeting to NPC in accordance with the mannose residues. These present results are

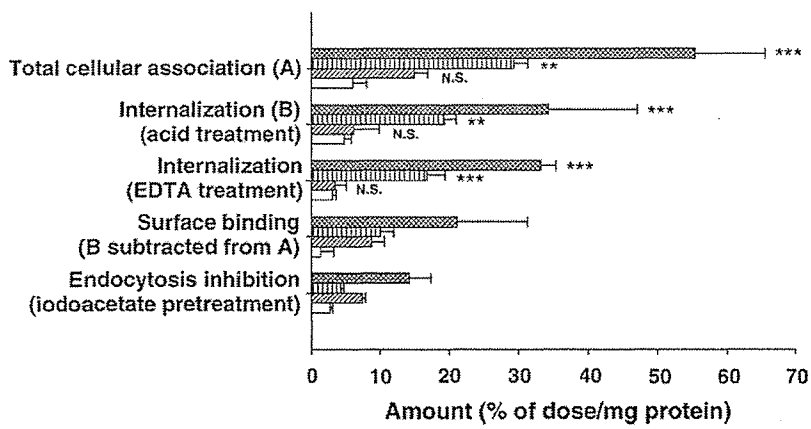

Fig. 5. Amount of emulsions associated with macrophages. Macrophages were incubated with Bare- (□), Man-2.5- (▨), Man-5.0- (▥) or Man-7.5- (▩) emulsions. After a 2 h incubation, the cells were washed with ice-cold PBS (total association), acetate pH 4 buffer or 20 mM EDTA in PBS in separate experiments. The difference in cellular association between EDTA or acid treatment and ice-cold PBS treatment was regarded as the amount associated with the cell surface. In another group, the cells were pre-incubated with HBSS containing 1 mM iodoacetate for 30 min prior to exposure to emulsions. Each value represents the mean±S.D. of three experiments. Statistically significant differences (**$P<0.01$, ***$P<0.001$) from Bare-emulsions in each group; N.S., not significant.

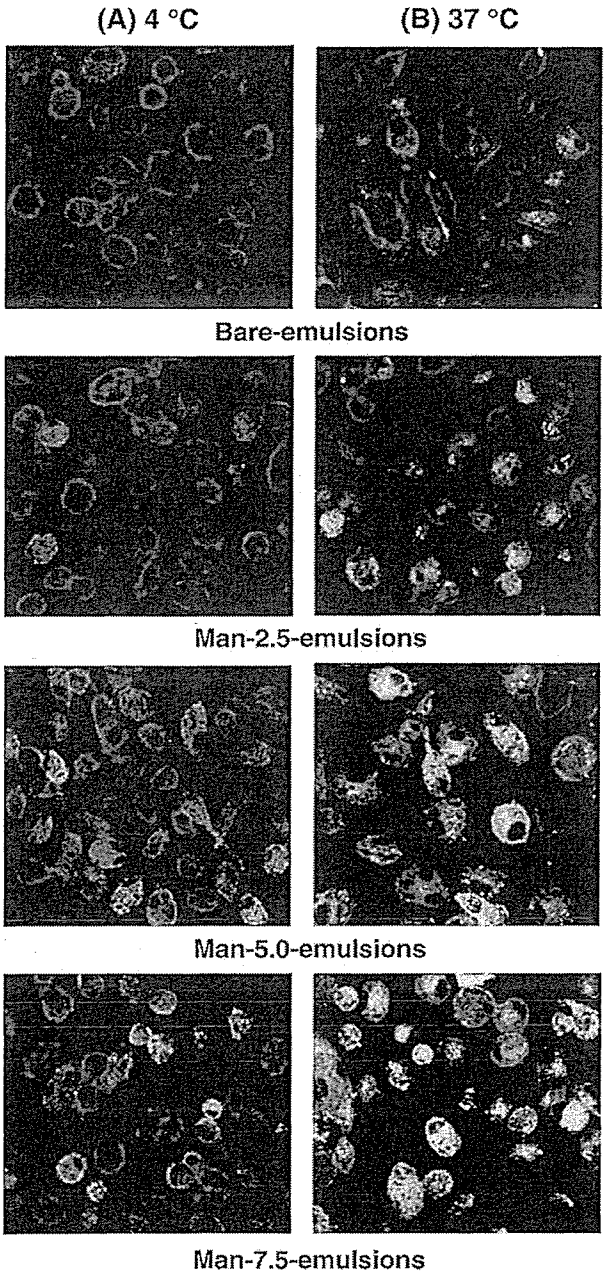

Fig. 6. Confocal microscopy images of binding and internalization of fluorescent PE-carboxyfluorescein emulsions by elicited macrophages. Macrophages were incubated with 0.12 mg/mL of emulsions at (A) 4 or (B) 37 °C for 2 h. The images are typical of at least three independent experiments.

similar to those of our previous study using galactosylated liposomes, which showed that the hepatic uptake was increased in proportion to the galactose density on the liposome surface via asialoglycoprotein receptors on PC after intravenous injection in mice [38].

To verify the uptake of Man-emulsions through mannose receptor recognition with respect to mannose density, in vitro uptake was examined in elicited macrophages which express mannose receptors on their cell surface. The uptake of Man-emulsions was considerably enhanced by increasing the number of Man-C4-Chol residues and significantly inhibited by an excess of mannan (Fig. 4) suggesting mannose receptor-mediated uptake which is in agreement with our previous studies that the in vivo uptake of mannose-modified emulsions and liposomes were significantly inhibited in the presence of Man-BSA [16,21]. The enhanced uptake of Man-emulsions corresponded to the results in the confocal microscopy study (Fig. 6). The in vivo and in vitro uptake experiments suggest that the mannose residues on the surface of Man-5.0- and Man-7.5-emulsions are enough to interact with mannose receptors, and trigger internalization. This trend agrees with our previous study involving galactosylated emulsions which showed that the uptake of galactosylated emulsions by HepG2 cells was enhanced on increasing the galactose density on the emulsions via an asialoglycoprotein receptor-mediated mechanism [39].

To investigate the uptake mechanism of Man-emulsions through a mannose receptor-mediated process in more detail, the cellular association of the emulsions was analyzed under different conditions. The inhibition of uptake of Man-emulsions by pretreatment with iodoacetate (Fig. 4) and reducing the temperature to 4 °C (Fig. 3B) suggests an energy-dependent endocytosis mechanism. After washing with acid and EDTA buffer, the total cellular association of Man-emulsions was reduced by both treatments suggesting calcium-dependent binding to mannose receptors which is in agreement with our previous study involving the hepatic uptake of Man-BSA after single-pass perfusion in rats [40]. The EDTA study showed that the amount of surface-bound and internalized Man-emulsions was similar to that in the acid treatment study. These identical results demonstrated that the amount of internalized Man-emulsions was significantly increased in proportion to the Man-C4-Chol content, while the corresponding surface-bound emulsions were slightly enhanced. The difference in the amount internalized could be explained by the effect of the mannose density on the surface of Man-emulsions that may be associated with the relative affinity of Man-emulsions for mannose receptors. These results lead us to believe that the improved internalization of Man-emulsions is, at least partly, due to the increased mannose density on their surface.

In this present study, the mean particle sizes of these emulsions were maintained at around 100 nm (Table 1), since the particle size appears to alter the physical stability during storage [21] and biodistribution [41,42]. The previous studies of the in vivo disposition of Bare-emulsions with a small particle size demonstrated that Bare-emulsions are largely taken up by PC after intravenous administration [41–43]. Consistent with previous reports, we observed that Bare-emulsions accumulated in the liver to a modest degree (Fig. 1) and were mainly localized in PC (hepatocytes) (Fig. 2), suggesting the selective uptake of Bare-emulsions by PC.

The uptake specificity of Bare-emulsions was examined in primary cultured peritoneal mouse macrophages. As shown in Fig. 3B, the low uptake of Bare-emulsions by macrophages at 37 °C agreed well with previous studies [44,45]. Granot et al. [44] and Sakurai et al. [45] investigated the cellular uptake of Bare-emulsions (with 60–80 nm in diameter) and showed that they were hardly taken up by J774 macrophage cell lines, which

express mannose receptors, in the absence of apo-E. These observations support the relatively low uptake of Bare-emulsions with small particle size by macrophages.

It is worthwhile using carriers with improved therapeutic properties for either systemic or local administration. The Kupffer cells, resident macrophages in the liver-NPC, secrete large amounts of proinflammatory cytokines after activation leading to cytokine-related diseases such as liver inflammation [46]. Since Man-emulsions selectively and highly accumulate in the liver-NPC, Man-emulsions containing anti-inflammatory drugs might improve low-dose treatment with less undesirable effects given by intravenous injection. Recently, the incidence of pulmonary tuberculosis has increased particularly with the AIDS pandemic, which has resulted in a huge number of deaths worldwide [47]. Besides the undesirable effects associated with long-term treatment, one problem associated with treatment is the failure of anti-tubercular drugs to penetrate into infected macrophages [48]. Accordingly, much effort has been directed toward the development of macrophage-selective targeting systems using a variety of carriers; however, their efficiency and specificity need further investigation. In this study, we have shown that Man-emulsions with 5.0% or 7.5% Man-C4-Chol are preferentially delivered to macrophages and effectively internalized into cells; therefore, they might be of use as a drug carrier for lipophilic drugs in the treatment of macrophage-related diseases.

In this present study, we evaluated the uptake characteristics of Man-emulsions by primary cultured mouse peritoneal macrophages. Previously, Muller and Schuber studied the uptake characteristics of neo-mannosylated liposomes composed of Egg phosphatidylcholine and cholesterol with mouse Kupffer cells and resident peritoneal macrophages and reported that neo-mannosylated liposomes were taken up by Kupffer cells and peritoneal macrophages in the same manner with nearly similar amount [49]. Although further studies are needed, this report might partly support the uptake characteristics of Man-emulsions by primary cultured peritoneal macrophages corresponding to that by primary cultured Kupffer cells.

5. Conclusion

Man-emulsions preferentially accumulated in liver-NPC after intravenous administration in mice based on the mannose density. Furthermore, Man-emulsions with a high content of mannose residues exhibited a higher binding affinity for macrophages and are extensively internalized compared with emulsions with a lower mannose content. These results strongly suggest that the mannose density of Man-emulsions play an important role in both efficient cellular recognition and internalization. These observations provide valuable information for the rational drug design of mannosylated carrier systems for efficient macrophage-targeting.

Acknowledgements

This work was supported in part by Grant-in-Aids for Scientific Research from the Ministry of Education, Culture, Sports, Science and Technology of Japan, and by Health and Labour Sciences Research Grants for Research on Advanced Medical Technology from the Ministry of Health, Labour and Welfare of Japan.

References

[1] I.P. Fraser, H. Koziel, R.A.B. Ezekowitz, The serum mannose-binding protein and the macrophage mannose receptor are pattern recognition molecules that link innate and adaptive immunity, Semin. Immunol. 10 (1998) 363–372.
[2] D.L. Lefkowitz, S.S. Lefkowitz, Macrophage-neutrophil interaction: a paradigm for chronic inflammation revisited, Immunol. Cell Biol. 79 (2001) 502–506.
[3] B. Friedman, K. Vaddi, C. Preston, E. Mahon, J.R. Cataldo, J.M. MacPherson, A comparison of the pharmacological properties of carbohydrate remodeled recombinant and placental-derived β-glucocerebrosidase: implications for clinical efficacy in treatment of Gaucher disease, Blood 93 (1999) 2907–2916.
[4] K. Shima, A.M. Dannenberg Jr., M. Ando, S. Chandrasekhar, J.A. Seluzicki, J.I. Fabrikant, Macrophage accumulation, division, maturation, and digestive and microbicidal capacities in tuberculous lesions: I. Studies involving their incorporation of tritiated thymidine and their content of lysosomal enzymes and bacilli, Am. J. Pathol. 67 (1972) 159–180.
[5] S.M. Moghimi, A.C. Hunter, J.C. Murray, Nanomedicine: current status and future prospects, FASEB J. 19 (2005) 311–330.
[6] Y. Takakura, M. Hashida, Macromolecular carrier systems for targeted drug delivery: pharmacokinetic considerations on biodistribution, Pharm. Res. 13 (1996) 820–831.
[7] G. Ashwell, J. Harford, Carbohydrate-specific receptors of the liver, Annu. Rev. Biochem. 51 (1982) 531–554.
[8] T.E. Wileman, M.R. Lennartz, P.D. Stahl, Identification of the macrophage mannose receptor as a 175-kDa membrane protein, Proc. Natl. Acad. Sci. U. S. A. 83 (1986) 2501–2505.
[9] M.E. Taylor, J.T. Conary, M.R. Lennaria, P.D. Stahl, K. Drickamer, Primary structure of the mannose receptor contains multiple motifs resembling carbohydrate-recognition domains, J. Biol. Chem. 265 (1990) 12156–12162.
[10] R.S. Haltiwanger, R.L. Hill, The ligand binding specificity and tissue localization of a rat alveolar macrophage lectin, J. Biol. Chem. 261 (1986) 15696–15702.
[11] B.L. Largent, K.M. Walton, C.A. Hoppe, Y.C. Lee, R.L. Schnaar, Carbohydrate-specific adhesion of alveolar macrophages to mannose-derivatized surfaces, J. Biol. Chem. 259 (1984) 1764–1769.
[12] Y.C. Lee, R.R. Townsend, M.R. Hardy, J. Lonngren, J. Arnarp, M. Haraldsson, H. Lonn, Binding of synthetic oligosaccharides to the hepatic Gal/GalNAc lectin: dependence on fine structure features, J. Biol. Chem. 258 (1983) 199–202.
[13] S. Takae, Y. Akiyama, H. Otsuka, T. Nakamura, Y. Nagasaki, K. Kataoka, Ligand density effect on biorecognition by PEGylated gold nanoparticles: regulated interaction of RCA_{120} lectin with lactose installed to the distal end of tethered PEG strands on gold surface, Biomacromolecules 6 (2005) 818–824.
[14] M.E. Taylor, K. Bezousaka, K. Drickamer, Contribution to ligand binding by multiple carbohydrate-recognition domains in the macrophage mannose receptor, J. Biol. Chem. 267 (1992) 1719–1726.
[15] S. Kawakami, J. Wong, A. Sato, Y. Hattori, F. Yamashita, M. Hashida, Biodistribution characteristics of mannosylated, fucosylated, and galactosylated liposomes in mice, Biochim. Biophys. Acta 1524 (2000) 258–265.
[16] P. Opanasopit, M. Sakai, M. Nishikawa, S. Kawakami, F. Yamashita, M. Hashida, Inhibition of liver metastasis by targeting of immunomodulators using mannosylated liposome carriers, J. Control. Release 80 (2002) 283–294.
[17] Y. Hattori, S. Kawakami, S. Suzuki, F. Yamashita, M. Hashida, Enhancement of immune responses by DNA vaccination through targeted